

A Wearable Pneumatic Device for Investigating
Ankle Inversion and Eversion in Human Gait

by

Andrew Barkan

A Thesis Presented in Partial Fulfillment
of the Requirements for the Degree
Master of Science

Approved April 2016 by the
Graduate Supervisory Committee:

Panagiotis Artemiadis, Chair
Hyunglae Lee
Hamidreza Marvi

ARIZONA STATE UNIVERSITY

May 2016

ABSTRACT

Human walking has been a highly studied topic in research communities because of its extreme importance to human functionality and mobility. A complex system of interconnected gait mechanisms in humans is responsible for generating robust and consistent walking motion over unpredictable ground and through challenging obstacles. One interesting aspect of human gait is the ability to adjust in order to accommodate varying surface grades. Typical approaches to investigating this gait function focus on incline and decline surface angles, but most experiments fail to address the effects of surface grades that cause ankle inversion and eversion. There have been several studies of ankle angle perturbation over wider ranges of grade orientations in static conditions; however, these studies do not account for effects during the gait cycle. Furthermore, contemporary studies on this topic neglect critical sources of unnatural stimulus in the design of investigative technology. It is hypothesized that the investigation of ankle angle perturbations in the frontal plane, particularly in the context of inter-leg coordination mechanisms, results in a more complete characterization of the effects of surface grade on human gait mechanisms. This greater understanding could potentially lead to significant applications in gait rehabilitation, especially for individuals who suffer from impairment as a result of stroke. A wearable pneumatic device was designed to impose inversion and eversion perturbations on the ankle through simulated surface grade changes. This prototype device was fabricated, characterized, and tested in order to assess its effectiveness. After testing and characterizing this device, it was used in a series of experiments on human subjects while data was gathered on muscular activation and gait kinematics. The results of the characterization show success in imposing inversion and eversion angle perturbations of approximately 9° with a response time of 0.5 s. Preliminary experiments focusing on inter-leg coordination with healthy human subjects show that one-sided inver-

sion and eversion perturbations have virtually no effect on gait kinematics. However, changes in muscular activation from one-sided perturbations show statistical significance in key lower limb muscles. Thus, the prototype device demonstrates novelty in the context of human gait research for potential applications in rehabilitation.

TABLE OF CONTENTS

	Page
LIST OF TABLES	iv
LIST OF FIGURES	v
CHAPTER	
1 INTRODUCTION	1
1.1 Overview and Background	1
1.2 Problem Statement and Scope	7
2 METHODOLOGY	8
2.1 Design Requirements	8
2.2 Conceptual Design	10
2.2.1 Design Analysis and Proof of Concept	16
2.3 Final Design	24
2.3.1 System Components	28
2.3.2 Fabrication and Assembly	31
3 EXPERIMENTATION	37
3.1 Actuation Testing	37
3.2 Preliminary Experiments	39
4 DISCUSSION	48
4.1 System Performance	48
4.2 Preliminary Observations	49
4.2.1 Effects on Muscular Activation and Gait Kinematics	49
4.2.2 Comparison of Inversion and Eversion	52
5 CONCLUSION	54
REFERENCES	56

LIST OF TABLES

Table	Page
2.1 Material Properties and Other Characteristics of Tubing Candidates. . .	18
2.2 Solenoid Valve Specifications.	25
2.3 TIP122 Transistor Specifications.	28
2.4 System Bill of Materials.	32

LIST OF FIGURES

Figure	Page
1.1 Anklebot System Actuation of Human Ankle ©2009, IEEE.	3
1.2 Experimental Setup Using Drop Mechanism.	5
1.3 Wearable Device for Perturbing Ankle in Sagittal Plane ©1995, IEEE.	6
2.1 Conceptual Diagram of Pneumatic Chamber Actuator Operation.	13
2.2 Diagram of Pneumatic Circuit for Control of Actuation.	15
2.3 Hardware and Setup for Actuator Proof of Concept Test.	19
2.4 Diagram of Final Design Hardware Components.	29
2.5 Electrical Schematic of Solenoid Control Board.	31
2.6 Models of Base Components in 3D Printing Software.	33
2.7 Full Assembly with Nonoperational Assembly.	34
2.8 Solenoid Assemblies in Pneumatic Circuit.	35
2.9 Electrical Hardware with Transistors and Arduino MEGA.	36
3.1 Filtered Angle Response Data for Inversion and Eversion	38
3.2 Eversion Actuation Response with Statistics.	39
3.3 Conceptual Illustration of Inter-Leg Coordination.	40
3.4 Experimental Setup and Subject Wearing Pneumatic Device.	42
3.5 Joint Angles of Unperturbed Leg for Representative Subject.	44
3.6 Joint Angles of Perturbed Leg for Representative Subject.	45
3.7 Muscular Activation of Unperturbed Leg for Representative Subject. ...	46
3.8 Muscular Activation of Perturbed Leg for Representative Subject.	47

Chapter 1

INTRODUCTION

1.1 Overview and Background

Most people do not realize the incredible complexity of their own body's gait mechanisms. Humans are capable of gathering and processing a significant amount of sensory information from their environment in order to generate walking motion. While sources of sensory feedback like vision are certainly essential to improving the robustness of human gait, one could argue that the body's tactile and proprioceptive senses are even more vital to the overall process of walking. Without a proprioceptive sense of leg location and configuration or input from tactile feedback and reaction forces, it would be extremely difficult to achieve efficient mobility over dynamic terrain. These are just a few examples of the different ways that we, as humans, use sensory data to control our gait mechanisms and interact with our environment.

Unfortunately, there is a large population of individuals who have gait impairment resulting in severely limited mobility. The inability to walk has serious consequences and can negatively affect an individual's freedom and independence. A major cause of gait impairment in humans is stroke. According to statistics gathered by the 2002 World Health Report, hundreds of thousands of people suffer a stroke every year, making it the leading cause of long-term disability in the U.S. Stroke is characterized by hemorrhaging in the brain, which can result in paralysis from damaged or severed neural connections. Rehabilitation studies have shown that the natural plasticity of the brain can be exploited to redevelop neural pathways that were impaired by stroke, provided that the correct training is implemented. As a result, many researchers have

been inspired to use and expand our understanding of human gait to help disabled individuals regain mobility through neurorehabilitation. The subject of training and rehabilitation for those suffering from gait impairment as a result of stroke is an essential topic in gait research that has the potential to greatly benefit the disabled community.

Over many years, researchers have learned a great deal about human walking motion and its associated control mechanisms. Because of these efforts, our understanding of human gait characteristics continues to grow; however, our ability to retrain gait motion in impaired individuals has not improved at the same rate. Gait rehabilitation through contemporary approaches can be a demanding and expensive process. Even with consistent and intensive treatment, methods like physical therapy often yield disappointing results.

Physical therapy clinics expend a significant amount of time and energy in each session in order to apply contemporary gait therapy techniques. Numerous sessions are required if one wishes to observe any positive results, which compounds the difficulty of these rehabilitation methods for both patients and clinicians. It is clear that the standard approach for rehabilitation lacks efficiency. From an engineer's perspective, the solution to problems involving highly repetitive tasks over long periods of time—such as those used in rehabilitation exercises—is robotics. Instead of employing physical therapists and technicians to prescribe rehabilitation techniques, a robot could be designed and implemented to perform the same exercises at a fraction of the effort and cost with much higher efficiency. The field of rehabilitation robotics has yielded a number of exciting possibilities for improving or replacing traditional gait therapy. Despite the seemingly clear advantages of robotics applications in gait rehabilitation, clinicians continue to report that both traditional physical therapy and robot-assisted models are showing dissatisfying results in gait improvement (Hornby

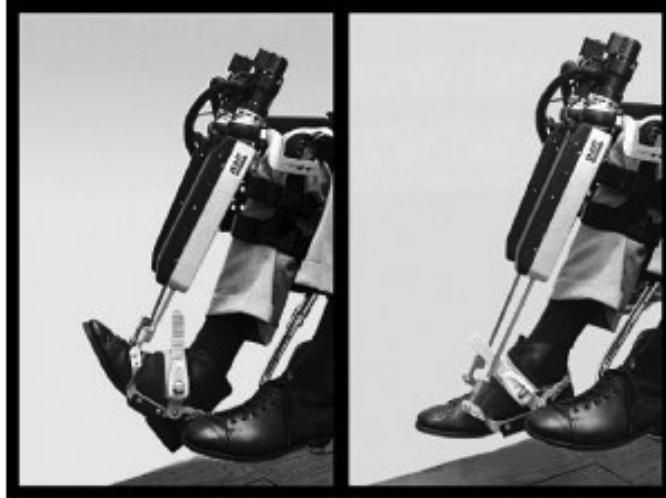


Figure 1.1: Anklebot System Actuation of Human Ankle ©2009, IEEE.

et al. (2008)). The failing in our approaches, therefore, must be due to a fundamental misunderstanding of the most effective way to rehabilitate gait in humans. This conclusion necessitates the development of technology that increases our ability to dissect and analyze the complex mechanisms involved in the process of walking.

While it is well understood that walking involves many parts of the body, the ankle plays a significant role in generating motion. Along with the hip, the ankle has been shown to contribute nearly half of the positive energy needed in typical walking gait (Farris and Sawicki (2011)). Naturally, researchers have identified the ankle as a critical component to our understanding of gait rehabilitation, and great research effort has been dedicated to investigating its characteristics. Fig. 1.1 shows a well-known example of a robotic system used to investigate and rehabilitate ankle functionality in humans (Roy *et al.* (2009)).

Besides being a source of power generation in human gait, the ankle must also have additional functionality in the form of sensing. The human leg is capable of gathering critical information about an environment through contact with a particular surface. Specifically, it is hypothesized that information such as stiffness, damping, grade,

and other surface characteristics can be transmitted through the proprioceptive and tactile sensing of human ankles. It then follows that dissecting the pathways of these signals and analyzing the associated responses seen in human gait is essential to the development of effective rehabilitation protocols. In the context of the rehabilitation of gait in stroke sufferers, the stimulus received from the environment during walking could be directly coupled to the regeneration of the associated neural pathways. Therefore, the investigation of the effects of surface characteristics on human gait has been a topic of great interest for researchers.

Feedback from the environment can potentially be gathered from many different characteristics of a particular type of surface. Certain environments that humans encounter might result in a change in surface stiffness or damping. In previous work, the effects of surface stiffness on human gait were investigated using novel treadmill technology (Skidmore *et al.* (2014)). The associated research demonstrated useful information about gait responses to stiffness perturbations that could be used in rehabilitation scenarios. These study also yielded new insight into inter-leg coordination mechanisms and their potential for rehabilitation applications. Surface grade could also have a significant effect on human gait. In fact, studies demonstrate that slope clearly influences gait outcomes like stride length and toe clearance (Prentice *et al.* (2004)). It is easy to imagine how an individual might have a natural reaction to adjust their gait kinematics or muscular activation in order to maintain balance over unexpected surface angles. This idea of exploring the effects of surface changes has yielded tremendous insight into the mechanisms of these responses, but the state-of-the-art technology used for these investigations still have not comprehensively addressed the role of the ankle in communicating feedback to human gait mechanisms. To get a sense of the needs of contemporary research approaches, it is necessary to consider some previous studies on the involvement of the human ankle

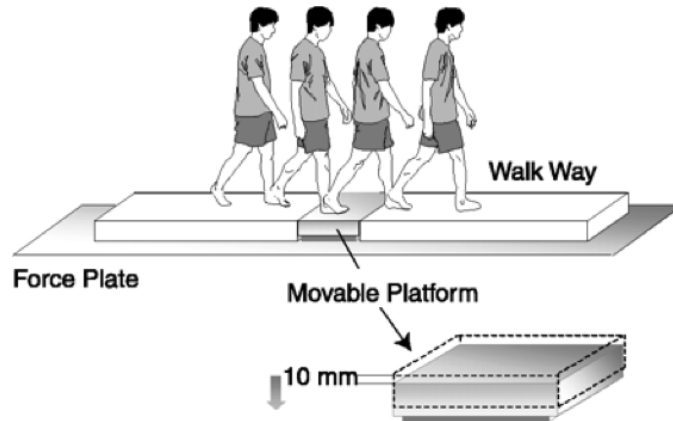


Figure 1.2: Experimental Setup Using Drop Mechanism.

in sensing and reacting to environments.

As mentioned previously, studies on the effect of surface characteristics on human gait have been prevalent in the gait research community. One such study used a moveable platform device capable of dropping a prescribed distance from an equilibrium surface height (Nakazawa *et al.* (2003)). An image of this device in the experimental setup is shown in Fig. 1.2. The results of this study showed the direct involvement of ankle muscular coactivation in the maintenance of stability after a surface drop.

However, the conclusions gained by this research can only be associated with surface drop perturbations, which have much different implications compared to a change in surface grade. A different approach employed the use of a novel wearable device capable of perturbing ankle dorsiflexion and plantarflexion, which is shown in Fig. 1.3 (Andersen and Sinkjaer (1995)). In this case, the system is designed toward investigating ankle responses to inclined or declined surfaces. While the application of this technology has covered part of the broader research domain related to joint rotations in the sagittal plane, any experiments conducted with this approach are incapable of addressing cases in which surface angle changes cause ankle joint rotations in the frontal plane of the body. Furthermore, experimental approaches that are capable of creating ankle inversion and eversion perturbations are often designed

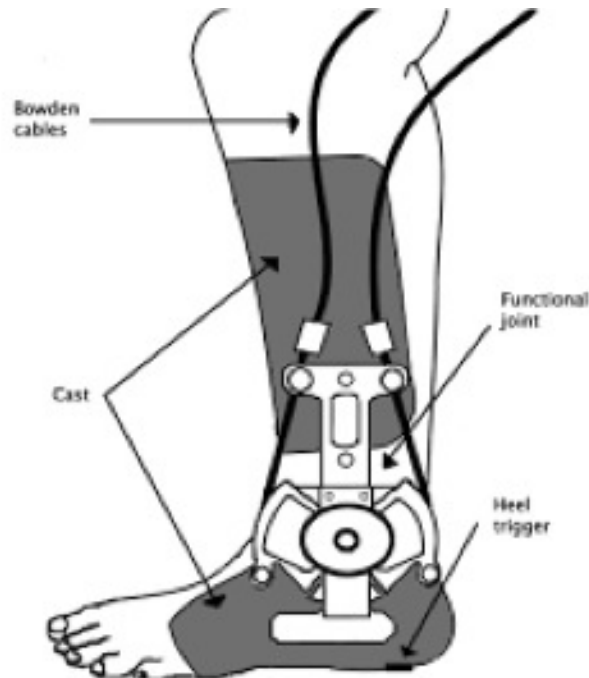


Figure 1.3: Wearable Device for Perturbing Ankle in Sagittal Plane ©1995, IEEE.

for use in stationary conditions (Nardone *et al.* (1990)).

The Anklebot (shown in Fig. 1.1) is one instance of a wearable robotic system that has the ability to perturb the ankle in both the sagittal and frontal plane degrees of freedom of the human ankle, and it is capable of applying these perturbations during the gait cycle. Wearable devices have the potential to greatly increase the ability of researchers to examine human gait in a robust and mobile way. A drawback of this system, and many other wearable robotic systems designed for investigating human gait, is that they can negatively influence natural stimulus when interfering with the body's motion or feedback. Typically, engineers design wearable robotic orthoses with actuators to actively impose changes in ankle angle. The important distinction between this approach and more natural scenarios is that the ankle should not be acted upon by coupled external forces. Instead, a more realistic perturbation would involve the ankle passively interacting with the environment. This type of distinction can have serious consequences for interpreting gait responses, and by effect,

the resulting conclusions for applications in rehabilitation.

The shortcomings of contemporary research technology and their associated studies call for a reevaluation of gait investigation approaches and a more thorough examination of the ankle's role in generating gait. More specifically, there is a need for the design of a system that can passively perturb ankle inversion and eversion during human gait in order to further develop our understanding of walking mechanisms.

1.2 Problem Statement and Scope

The design of wearable robotic systems for applications in gait investigation is a challenging problem because it lies at the intersection of a variety of design constraints such as limitations on weight, power, size, functionality, and even ergonomics. It becomes even more difficult when considering the added requirement of acting passively on the ankle. The problem statement and goal of this research is to design, build, and implement a wearable device for investigating the effects of ankle inversion and eversion in human gait in an effort to more completely characterize the human body's response to changes in surface grades. The hypothesis is that perturbing ankle inversion and eversion will elicit characteristic muscular activation and changes in kinematics as a result of underlying balance mechanisms.

To reduce the complexity of this design problem, the scope will be limited to designing a system that can actuate the ankle in the frontal plane. This is due to the fact that the effects of surface inclinations and declinations have been characterized to a greater extent in previous research. Because of the results shown by previous research in exploiting inter-leg coordination mechanisms, a similar approach will be adopted in this study as well. The goal of the system will be to apply perturbations to one side of the body during gait while measuring muscle and joint reactions on the contralateral leg.

Chapter 2

METHODOLOGY

2.1 Design Requirements

In order to tackle a difficult design problem, one must first define the design requirements and constraints to be met. As discussed previously, the primary purpose of this device will be the investigation of ankle inversion and eversion in human gait. In achieving this goal, the design must extend beyond the scope of contemporary technology in other aspects as well. The following list summarizes the most critical design requirements for the development of this system based upon the needs of the research applications discussed previously.

1. Capable of imposing ankle inversion and eversion.
2. Acts passively on the ankle.
3. Wearable and ergonomic.
4. Low weight and small size.
5. Does not impede or negatively affect natural gait.
6. Safe and consistent in operation.

This list will be useful as a guideline for determining the direction of the design, so it is important to review them and understand why they are critical to the success of the resulting system.

The ability of the system to impose ankle inversion and eversion is the main motivation behind embarking on this design process. Therefore, all aspects of the system must accommodate the actuation of the ankle in the frontal plane. This requires the consideration of any potential degrees of freedom and the possibility of obstructions. Secondly, the design must not directly actuate the body. In other words, the method of perturbing the ankle should not act to create an independent force on the subject's body in order to produce the desired motion. Instead, the subject must experience the perturbation as a passive part of the simulated environment. This requirement will be particularly challenging to achieve, as most contemporary systems rely on active methods of actuation. Another important aspect of the desired system is that it should be wearable. A wearable system brings with it a number of associated constraints because of the involvement of human factors. If the proposed design is uncomfortable or unaccommodating to human movements, there will be negative effects on the resulting gait motion, which could be detrimental to rehabilitation efforts. It then follows that coupled aspects of the design such as weight and size should be limited in order to meet wearability requirements. Finally, the proposed design must always be safe and predictable in operation so as to not endanger human subjects. The importance of this last requirement is made even more pertinent by the fact that this system will likely be in contact with the subject at all times during the experiment.

With the requirements now adequately defined, the preliminary design of the system can start to take shape through the satisfaction of these same constraints. The next step will involve developing the form and basic components for this system in the conceptual design stage.

2.2 Conceptual Design

The challenges with creating any effective design arise with the combination of satisfying design requirements and optimizing free design parameters. Since the requirements are now known, the remaining aspects of the design not driven by constraints are considered free. In the context of this problem, there are many ways in which to passively impose a change in angle on the ankle, but there likely exists an optimal approach that satisfies the requirements given in the previous section.

Deviating from the contemporary approach of active perturbations on the human ankle will rely on some clever problem solving. First, one must investigate how the human body perceives the changes in inversion and eversion angles of the ankle. To avoid introducing unnatural stimulus, the system design should replicate this process as accurately as possible. When encountering an uneven grade in a particular surface, the ankle is turned as a result of the normal forces arising from planting the foot. This leads to the conclusion that the desired system must change the effective interface between the bottom of the foot and the surface upon which it is planted. If the relative angle of this interface can be controlled or actuated, then perturbations of ankle angle can be simulated naturally without negatively affecting the feedback that the body receives. The problem can now shift to the process of determining an effective vehicle for this actuation.

This application requires a method of actuation that accommodates the weight and size limitations while having high enough energy density to effectively impose ankle angle changes through the bottom of the foot. In addition, the actuator type must conform to the human subject in such a way that natural motion remains unaffected. To solve this problem in the design of wearable actuators, cable driven systems are commonly used. Actuator options include high efficiency electromechanical mo-

tor solutions as well. Unfortunately, these types of actuation conflict with one of the aforementioned requirements because they are more suited for active applications where force is prescribed directly to the body. Furthermore, these actuators typically contain or require rigid mechanical components, which could cause problems when being implemented into a wearable device that is intended to conform to the body. In order to solve this problem, it will be useful to conduct a more thorough analysis of the desired motion created by the actuation.

As stated before, the method of perturbing ankle inversion and eversion passively will involve controlling the interface between the bottom of the foot and a given ground surface. Since one of the requirements of the system is wearability, the device must operate in a space constrained to the area surrounding the foot. It is possible to design a wearable mechanism that can be fastened to the bottom of the foot, which adjusts the angle of the surface that makes contact with the ground. A device fastened to the foot would not distort the perception of a natural situation because humans are conditioned to having shoes fastened to their feet during gait on a daily basis. In this way, the mechanism could make flat and even contact with the ground while transmitting a change in angle through the bottom of the foot resulting in actuation of the ankle joint. By assuming this design approach, additional size and weight limitations are introduced to the problem. Essentially, this controllable interface between foot and ground must occupy approximately the space of the sole of a shoe in order to be reasonably ergonomic and natural to the user. As such, many of the aforementioned actuator solutions can be eliminated as potential options.

One possibility for actuation that is less common in wearable applications is pneumatics. Pneumatics are often avoided due to the fact that they are notoriously difficult to control. However, a pneumatic actuation solution could offer some key advantages that might cater to the specific design requirements of this problem. Pressure-driven

actuation has the ability to be flexible, which is extremely useful in wearable design applications because of the high fidelity of movement inherent in many aspects of the human body. For example, shoes are frequently made of extremely flexible rubber material in order to accommodate the numerous joints and degrees of freedom of the human foot. Using flexible, pressure-driven systems would allow the foot to maintain its range of motion without sacrificing space. This natural compliance is also useful when the full weight of a human subject is applied to the device. While an elastic pneumatic component may flex, it is less likely to be damaged by this loading. An electromechanical device limited to similar size and weight of this application would be unable to withstand the same loading without breaking.

The reason pneumatic systems are difficult to control accurately in a system is largely due to issues with accurate pressure measurement and the natural compressibility of air at working pressures. These limitations may cause issues for the consistent control of a pneumatic device. In order to combat these problems, the design scope can be reduced to that of an open-loop approach involving only two states: non-perturbation and perturbation. Although this may limit the functionality of the device in controlling specific ranges of inversion and eversion angle perturbation magnitudes, it will significantly increase the system's simplicity and resultant consistency in operation. After conducting this analysis of the design space for actuation, it has become clear that the most suitable choice is pneumatic actuation. This option will provide the system with the optimal weight, size, and power requirements for the application. With this conclusion, the design can progress toward the consideration of potential pneumatic actuator configurations and geometries for accomplishing the desired motion under the foot of the subject.

The next part of the process will require analyzing the desired motion in reference to potential pneumatic actuator configurations within the design space defined previ-

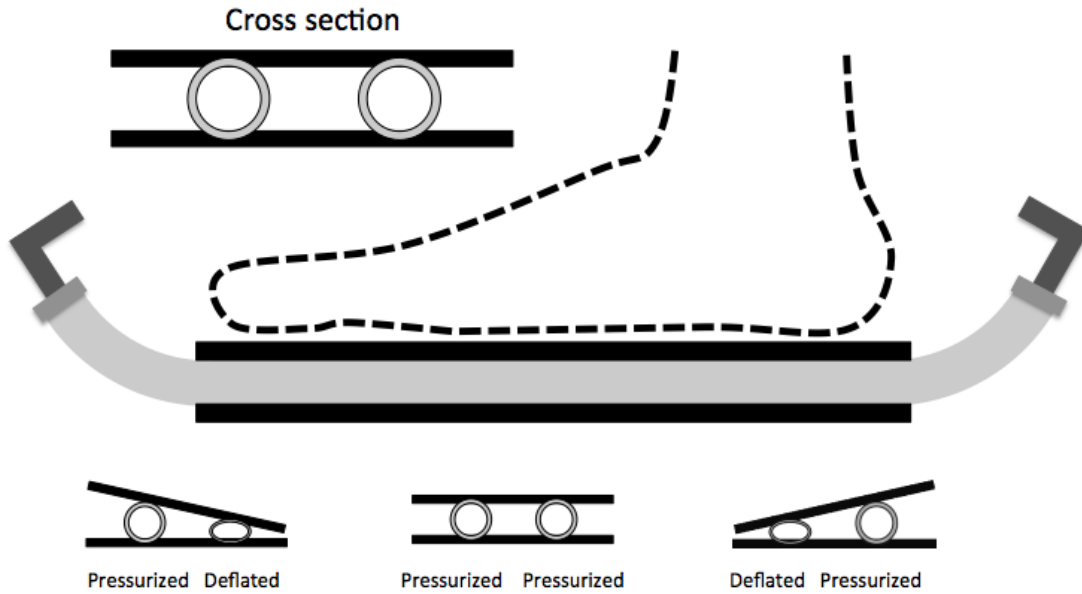


Figure 2.1: Conceptual Diagram of Pneumatic Chamber Actuator Operation.

ously by the requirements. A common air-driven actuator adopted by many robotic applications is the pneumatic cylinder. This type of actuator would be ill-suited for this application because of the limited potential stroke length of the cylinder based on the maximum allowable distance between the subject’s foot and the ground. For the design of this system, inspiration from soft robotics applications can be applied. By exploiting the expansion of a pressurized elastic chamber, the bottom of the foot can be driven up and down to simulate surface angle perturbations. The images in Fig. 2.1 demonstrate a possible geometry and configuration for elastic chambers that can be pneumatically activated to create the desired motion in the ankle.

As shown in this figure, a very simple geometry can achieve the desired perturbation effectively with the use of two pneumatic chambers secured between two rigid surfaces. The adoption of this simple configuration does have drawbacks. For instance, the parallel actuation of this design may result in slight vertical translation of the top surface due to the compressibility of the fluid. It could be assumed, however,

that the magnitude of this vertical displacement from compression is comparable to the movement caused by the compliance of a typical rubber sole. Essentially, this source of error could potentially be negligible in relation to natural conditions. One might also argue that the suspension of a rigid surface on parallel compressible air bladders could cause undesirable instability in a subject's gait. These types of factors will be investigated in a subsequent section when an actuator proof-of-concept assembly is tested.

In the design approach discussed above, the surfaces that secure the inflatable tubes are also important to consider because they distribute pressure from the weight of the body across the actuators. In doing so, the top surface prevents transmission of unnatural tactile forces due to the uneven geometry and variable compliance of the tubes. There must be a fine balance between rigidity of the surface and flexibility of the entire device. The device surface must simulate a solid flat surface but still be compliant enough to conform to the foot's motion throughout the gait cycle. Primarily, the critical movement of joints in the foot itself is bending in the sagittal plane across the ball of the foot and the arch. By design, the pressurized chambers will be able to flex with movement along this degree of freedom, but design consideration must be given to how the securing surfaces of the device will allow this motion. Fortunately, an easy solution exists that will also afford the system added functionality. Splitting the top surface into a toe section and a heel section while maintaining the connection of the two sides through the pneumatic tubes will create a joint at the ball and arch of the foot. This gap can be adjusted by sliding the two halves closer or farther apart along the length of the actuator tubes, making it capable of fitting a wider range of foot sizes with more conformance. The system is also made more modular by this change so that different surface geometries for toe and heel components can be interchanged to create multiple configurations of the assembly.

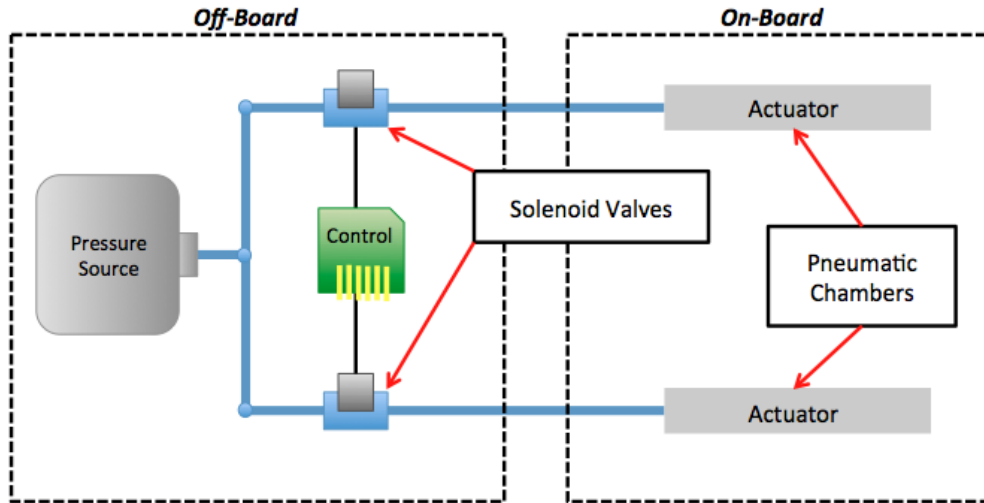


Figure 2.2: Diagram of Pneumatic Circuit for Control of Actuation.

A significant aspect to the design which hasn't been covered is the development of a pneumatic circuit layout and a control scheme for actuating the individual air chambers. The clear choice for open-loop pneumatic control applications is a solenoid-driven directional air flow valve. With solenoid valves, the flow of air to the chambers can be directly controlled through digital signals. Fig. 2.2 gives an illustration of the basic components of a simple pneumatic circuit that could be implemented to control the two actuators. This diagram also illustrates the grouping of the pneumatic circuit components into off-board and on-board locations. To reduce the weight of the system, the on-board components must be limited. Determination of a type of pressure source will be dependent on further analysis of the expected system performance, which will occur in the next section.

Solenoids usually require both a voltage source and a control signal sent by some external system. Since this device will be employed in research experiments, the control system should be able to interface and cooperate with the other components of the experimental setup in order to facilitate experimental operation and data processing. Arduino platforms represent cheap and reliable ways for either operating inde-

pendently with limited processing power or communicating with computers through serial commands. Although it is probably unnecessary to have the controller on-board as a part of the wearable system, Arduino controllers are also exceptionally small and light, making them highly conducive to wearable applications. In the case of this design, the solenoids will be off-board, so there is no reason to have the controller on-board. As shown in Fig. 2.2, the solenoids will be able to control the pressure distribution to the two actuators worn on the foot through air hoses, which allow the other components of the system to remain off-board.

Further development of the design characteristics of the system will require more analysis into the key physics behind its method of operation and closer examination of the component selection. The conceptual design aspects that were developed in this section will serve as a framework for the more detailed design phases to come.

2.2.1 Design Analysis and Proof of Concept

The previous section was critical in determining a direction for the design of this wearable pneumatic system for perturbing ankle inversion and eversion. However, the design must mature significantly, and analysis must be conducted in order to ensure confidence in the success of its operation. First and foremost, the decision to use a pneumatic method of actuation and the associated configuration discussed earlier are in need of characterization.

A driving factor of the design of pneumatics is the required operating pressure. The application of this system does not require variable pressure, so the goal will be to determine an adequate range of static pressure based on the known conditions of operation. One of the initial considerations that was made when choosing pneumatic actuation was the possibility of compressing the air chambers, resulting in instability or undesired vertical displacement. The operating pressure must be chosen such that

the device will withstand the full compressive load of the subject's weight during the gait cycle and for many repetitions. Since the actuator tube is expected to maintain its shape under pressurized conditions, the expansion of the tube material in this state will be neglected.

One problem that has not been addressed at this point is the possibility that the subject's weight could have a large influence on the pressure inside the actuator chamber. To analyze this problem, it might be useful to examine a similar engineering scenario: the design of bicycle tires. Bicycle tires are elastic pressurized chambers with approximately cylindrical cross sections that undergo loading from the weight of a human just like the actuator design in question. In response to the loading of a human rider, an adequately pressurized bicycle tire will usually experience minimal compression. Bicycle tires are typically filled to a pressure of anywhere between 30 psi to 130 psi, depending on the weight of the rider, type of tire, and type of bicycle. It is therefore safe to assume that the operating pressure of the tubes used in this application will be on the same order of magnitude as long as similar material properties are chosen.

The explicit analysis of the theoretical pressure change under the loading of a human subject turns out to be quite complex because of the flexibility of the chamber. Instead, a proof-of-concept test on a simulated actuation testbed could help gain the required information about potential pressure ranges in addition to a number of other outcomes related to understanding the expected operation of the system. This test will also be an opportunity to explore potential tubing material choices for the actuator chambers. After some research into common material properties for pressurized tubes and also some consideration of the required characteristics, two material candidates were identified. Table 2.1 shows the relevant properties of the two tubing candidates. The critical property for determining the deformability

Table 2.1: Material Properties and Other Characteristics of Tubing Candidates.

Material Type	ID (in)	OD (in)	Hardness (Durometer)	Hardness Rating	Maximum Pressure (psi)
Tygon PVC	0.625	0.875	65A	Soft	160
Silicone Rubber	0.625	0.965	60A	Soft	100

of the material is the hardness measurement using the Shore durometer scale. It should be noted that both candidates are relatively close in the respective hardness properties, but the difference in material choice has a clear affect on the maximum internal pressure rating. It is expected that the proof-of-concept test will reveal other important design considerations relating to material choice that have not been identified up to this point.

The proof-of-concept test is expected to answer a range of questions that are critical to moving forward with the design. A list of these questions can be seen below.

1. What range of pressures can support minimal deflection under the compression of body weight?
2. How much does body weight contribute to the internal pressure of the tubing?
3. How do the different air chamber material candidates respond to compression when open to atmosphere?
4. How do the different air chamber material candidates compare qualitatively in terms of their deformability?

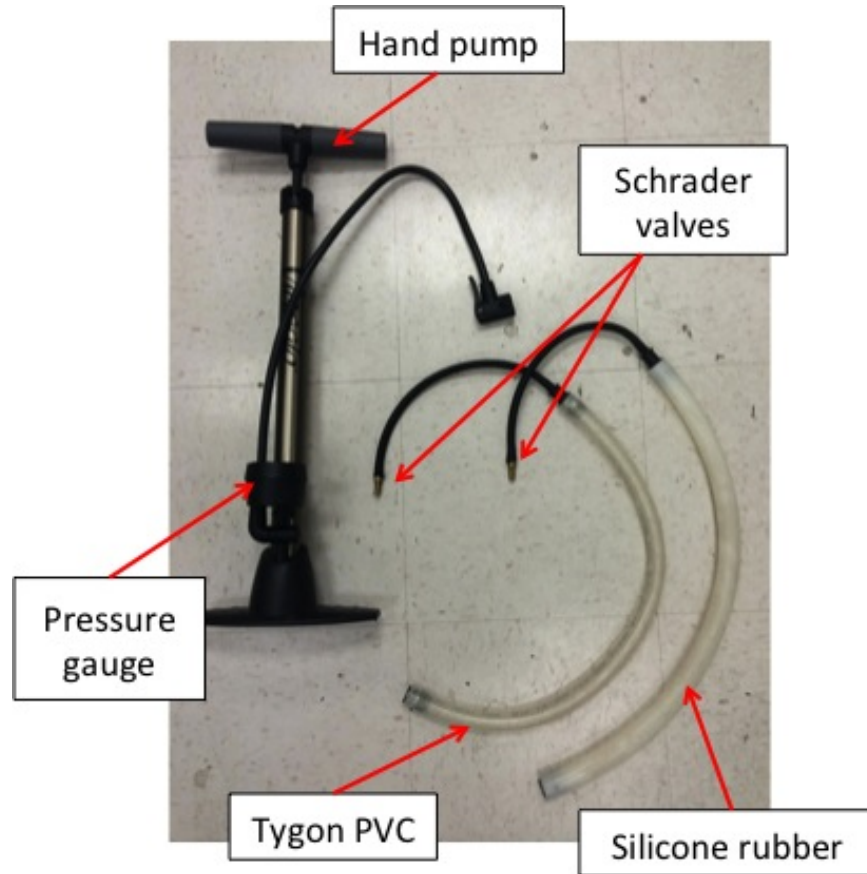


Figure 2.3: Hardware and Setup for Actuator Proof of Concept Test.

The first question in the list above will drive the selection of all associated pneumatic components by determining a required pressure rating. For example, the solenoid valve will have to be chosen based on the pressure capacity. If the pressure in the system exceeds this rating, the system would be unreliable and potentially hazardous in operation. This also applies to the other components that transmit pressure through the system, such as hoses and tubing interfaces. Pneumatic components will be dependent upon each other for size compatibility as well, which introduces another free design parameter. The proof-of-concept test must definitively show whether or not the weight of a human subject can significantly increase the internal pressure of the tubing. If it does, provisions should be made in the design to accommodate fluctuations in pressure throughout its operation.

Figure 2.3 identifies the different components of the proof-of-concept test hardware. The two material candidate tubes have been fashioned into closed chambers with an inlet tube. The inlet tubes are fitted with Schrader valves in order to allow the manual control of pressure by way of a standard bicycle pump. By using a bicycle pump, a reasonable range of internal pressure can be achieved while simultaneously measuring pressure data with the gauge. The results of the proof-of-concept experiment led to some critical conclusions about the direction of the design. These conclusions are listed below.

1. The most suitable candidate for this application is the clear tygon material tubing, which was determined based on qualitative deformation.
2. A reasonable operational pressure range for maintaining tubing shape under the compression of subject load is between 40 and 50 psi.
3. Increases in internal pressure from the subject load were not observed and can be considered negligible in static conditions.
4. Accommodations must be made for axial expansion and contraction of tubing with pressure changes.
5. The tubing can fully deform when opened to atmospheric pressure conditions.

As seen in the list above, a material candidate has been identified as the most suitable type of tubing for the application as an actuator in the system. This determination was made based on the qualitative ease of deformability of the materials, with clear tygon being much more compliant than the silicone rubber. The adequate pressure range was determined by using the hand bicycle pump to investigate the lowest possible pressure needed to support a subject's weight in stance. The range

from 40 to 50 psi is a common working range of pressures for low power pneumatic components, so it should facilitate the selection of parts that fit specifications. This low pressure range makes it possible to design a factor of safety into the system as well. Results also demonstrate that subject weight is not enough to impose changes in internal pressure. The fourth conclusion regarding the expansion and contraction of the tubes in the axial direction will not be an issue since the securing surfaces of the device are separated at the arch of the foot, allowing for translation. Finally, the tests determined that the tubing will fully deform as a result of the subject's weight when the circuit is opened to atmospheric pressure conditions. This last conclusion is critical because it confirms the ability of the proposed system to passively create surface angle perturbations.

Following the proof-of-concept testing, the design has matured significantly; however, the new developments also make it possible to gain an understanding of the expected system performance based on current design parameters. For instance, the actuation approach and configuration have been identified, so it is important to conduct a preliminary analysis predicting how it might operate in nominal conditions with proposed parameters. A desired output for angular displacement in the frontal plane of the ankle must not reach values that could result in subject injury. Based on typical ranges from literature, the minimum inversion or eversion angle to cause injury is around 30° ; therefore, the system should operate such that the perturbations remain below this value (Begeman *et al.* (1993)). Using nominal values of foot width and the diameter of the previously chosen tubing candidate, a theoretical maximum angular displacement can be calculated. Depending on the finalized dimensions of the width of the device's surface, the maximum angular displacement should vary between 10° and 20° . Now that the static performance of the system has been characterized in theory, focus can be shifted toward understanding the expected transient

response of the actuation.

The proof-of-concept showed that the tubing can be deformed completely under the loading of a human subject when opened to atmospheric conditions, but the rate at which the displacement occurs has not been determined. To analyze this outcome, the rate of air exhaustion from the tube under compressive load can be determined and used to find the amount of time it would take to deflate the volume. It turns out that this problem can be approached in a number of ways, but the easiest way to approximate the velocity of the exiting air is to employ Bernoulli's equation in the static case. For this analysis, the effects of the weight of the subject will be neglected, but it should be noted that the force from the foot will actually increase the air exhaust speed because the chamber will be open to the atmosphere instead of being sealed, allowing the volume to decrease as a result of the external compression. This distinction is important because it distinguishes this case from the proof-of-concept test in which the effects of the subject's weight were determined to be negligible. This assumption also prevents the involvement of transient changes in volume, which can complicate the calculation greatly. It should be noted that once the pressure is equalized with atmospheric pressure, the mechanism driving the exhaustion of air is the reduction in volume-to-surface-area ratio.

In the case of this problem, only an approximation is needed, so many simplifying assumptions will be made in regard to the properties of the fluid and the transient behavior. The pressure, density, and outlet velocity will all be assumed to be constant with an initial minimum pressure of 40 psi. Bernoulli's equation between a point within the tubing and a point at the outlet can be simplified in the following way.

$$P_1 + \frac{1}{2}\rho v_1^2 + \rho gh = P_2 + \frac{1}{2}\rho v_2^2 + \rho gh \quad (2.1)$$

$$P_1 - P_2 = \Delta P = \frac{1}{2}\rho v_2^2 \quad (2.2)$$

By rearranging this equation, the velocity at the outlet can be determined.

$$v_2 = \sqrt{\frac{2\Delta P}{\rho}} \quad (2.3)$$

Then, the velocity can be used to calculate the volumetric flow rate out of the tube at this particular pressure. Nominal values for dimensions in the system can be taken to determine the outlet area and a tubing volume in order to find the change in time. For this calculation, the diameter of outlet will be 0.25 in and the length of the tubing will be 12 in.

$$Q = v_2 A \quad (2.4)$$

$$\Delta t = \frac{V}{Q} = 0.08 \text{sec.} \ll 1 \text{sec.} \quad (2.5)$$

The result of this calculation only shows the amount of time necessary to reach equilibrium pressure with atmosphere. Explicitly calculating the rate of flow due to external compressive forces and changes in volume-to-surface-area ratio requires the implementation of Navier-Stokes, and it will be considered beyond the scope of this analysis. It should be expected that the increase in response time will be significant depending on the area of the exhaust outlet.

As shown above, the total time over the change in pressure and full evacuation of the tube is likely to be much less than a second. These calculations increase the confidence in the proposed design. Based on this analysis, the response should certainly be fast enough in order to be perceived as a perturbation to the human subject. Thus, the system is expected to be capable of creating angular perturbations with effective response times.

At this point, enough analysis has been conducted on the preliminary design to support an understanding of its expected operation. The next stage will require the selection of final components and transitions into fabrication and assembly of the device.

2.3 Final Design

The previous sections were important in analyzing and identifying a general approach to the design of this wearable device for perturbing ankle inversion and eversion. However, the definition of specific dimensions, parameters, configurations, and components has not been achieved yet. The subject of this section will be the determination of a suitable final design for fabrication, assembly, and eventual testing. In the process of determining the final design from a preliminary design, one must begin to synthesize the most critical components first. From earlier, the design of the pneumatic actuators has progressed significantly based on the analysis of its expected performance.

The material candidate chosen for the design of the actuator chambers is clear tygon because it demonstrated the best performance and properties in proof-of-concept trials. The size of this actuator is constrained by the analysis conducted on maximum angular deflection, so it will have an inner diameter of 0.625 in. Its length will have to accommodate a range of potential foot lengths since the proposed design of the securing surfaces is modular and can slide to make the device shorter or longer if necessary. The maximum length of a typical human foot should not exceed 15 in; therefore, the actuator should be slightly longer than that in order to have margin.

Other components that are necessary in the design of the actuators are those that transmit and direct the pressure. Since these tubes are elastic, the clear choice for transitioning between different types of tubing is barbed fittings. Plastic barbed

Table 2.2: Solenoid Valve Specifications.

Valve Type	Solenoids	Voltage	Pressure Rating
3 Port, 2 Position	Double	24V DC	29 - 145 psi

fittings can be found readily and in many different sizes, and they are extremely lightweight, making them excellent candidates for this design. Even though they are plastic, these barbed fittings are rated to high internal pressures and can withstand the chosen operating pressure with a high safety factor. In addition to these fittings, hose clamps should be used on the outside of the tubing to create a tight seal on the elastic material, which will prevent slipping.

To control the flow of air to these actuators, solenoid valves will be employed. This part of the design process of a pneumatic circuit can be challenging because there are so many different types and configurations of solenoid valves that could be used to accomplish the goal. The requirements from this design are that the solenoid valve configuration must be able to independently control air pressure to each of the two actuator chambers, and they must be able to operate at the chosen pressure range of 40 to 50 psi. With these considerations, a suitable choice of solenoid valves is a three-by-two way double solenoid valve. The specifications of this part is shown in Table 2.2. Using two of these solenoid valves—one for each actuator—it should be possible to control the independent distribution of pressure.

Another design aspect to tackle is the designation of a source of air pressure for the system. Fortunately, the facilities at Arizona State University have pressurized air outlets installed in many of the labs. These outlets supply steady pressurized air at roughly 40 to 45 psi, which is perfect for our desired application. The outlets typically use a 0.25 in quick-disconnect interface for attaching pressurized air hoses.

This fitting is also common for portable air compressors used by pneumatic tools. If this fitting and size of air hose is used for the design of the wearable pneumatic system, then it could be used in conjunction with either pressurized air wall outlets or compressors.

The next part of this process involves the design and modeling of the securing surfaces of the pneumatic shoe device. This component will act as the interface between the subject's foot and the actuators, so it is important that considerations are made for comfort as well as functionality. From previous discussions on the design of the surfaces, it is known that there will be both a heel and a toe section comprising the top surface of the shoe device. Each of these parts will need to be secured safely to the actuator tubes in such a way that the actuation is effectively transmitted. To accomplish this, the surfaces will be made with flat bottoms and shallow channels for securing the cylindrical actuators in place. These grooves will help prevent sideways movement of the actuators during operation. The actuators can be fastened to the shoe surfaces by creating slits along the outsides of the grooves that pass through to the top, allowing the placement of adjustable zip ties.

Designing the profile of the surface is also essential. In order to make it as unobtrusive and conforming as possible, the shape should resemble that of a typical shoe in which the front toe piece has wider surface area and the back heel piece tapers to a rounded end. Nominal measurements of different types of shoes were used to guide the dimensioning of this profile so that a wide range of subjects could fit in them, keeping in mind that the overall length can be adjusted via the inherent modularity of the surfaces. To keep the shoes of the subject secured to the device, the geometry can be designed with short walls along the perimeter of the surfaces to prevent slippage of the shoe. These walls will be more pronounced at the ends near the heel and toe because these regions are subjected to the highest relative displacement as a result of

the foot's flexion and extension.

Fastening the shoe device to the foot of the subject requires inspiration from common footwear, such as sandals. Velcro straps make it possible to maintain weight and size restrictions while accommodating different shoe types. Also, velcro straps are surprisingly strong and can be purchased with buckles to cinch across the subject's feet and secure them tightly onto the shoe device. These straps will pass through slits in the surface of the pneumatic device.

Since the length of the actuators is fixed and the relative locations of the heel and toe components of the surface are not, the actuators will be protruding from either the front or the back of the device. The grooves under the bottom of the foot for holding the actuators can be extended to curve around the toe and around the heel. Additional slit locations for securing the tubes can be added to the pronounced toe and heel walls. This method allows the actuators to conform better to the foot without obstructing its motion during the gait cycle.

The last item to address in the final stages of the design is the cooperation of electrical components. In particular, a circuit must be devised for controlling power to the solenoid valves. It would be preferable that the system be controllable from a computer so that the experiments can be coordinated with data collection. As shown in Table 2.2, the solenoid valves operate at 24V DC, but this voltage is too high for an Arduino to handle. The standard electrical component for controlling high power inputs is the transistor. By creating a circuit with transistors connected to each solenoid, an Arduino can be used to control the supply of power through the transistors from an independent DC power source. With the power specifications defined by the solenoids, a suitable transistor selection would be the TIP122. Specifications for this component are given in Table 2.3. For an additional safety measure, diodes should be placed in parallel with the solenoids to prevent any potentially damaging

Table 2.3: TIP122 Transistor Specifications.

Transistor Model	Type	Max. Voltage	Max. Current
TIP122 Transistor	NPN	100V	5A

back current from the solenoid operations.

At last, the design has matured into a final configuration with all components selected. Before fabrication and assembly, it is important to review the entire system and understand the roles of each component in order to ensure that all requirements have been sufficiently covered.

2.3.1 System Components

The various stages of the design process have yielded the finalized prototype design of a wearable pneumatic device for perturbing ankle inversion and eversion in human gait. Based on preliminary analysis of its expected operation and selection of components, the system should be successful in creating frontal angle perturbations in the human ankle during gait.

Each component of the system is designed for a specific function that is essential to the overall successful operation. First, the hardware components should be reviewed. Fig. 2.4 shows a basic diagram of the most important hardware components—and several of the electrical components—in their finalized configurations. The list below corresponds to the number labels in the diagram.

1. Highlights the items contained in the wearable portion of the pneumatic shoe device including the actuators and the securing surface components.
2. Elastic tube actuators made from clear tygon tubing that can independently actuate to create inversion and eversion ankle angle perturbations during the

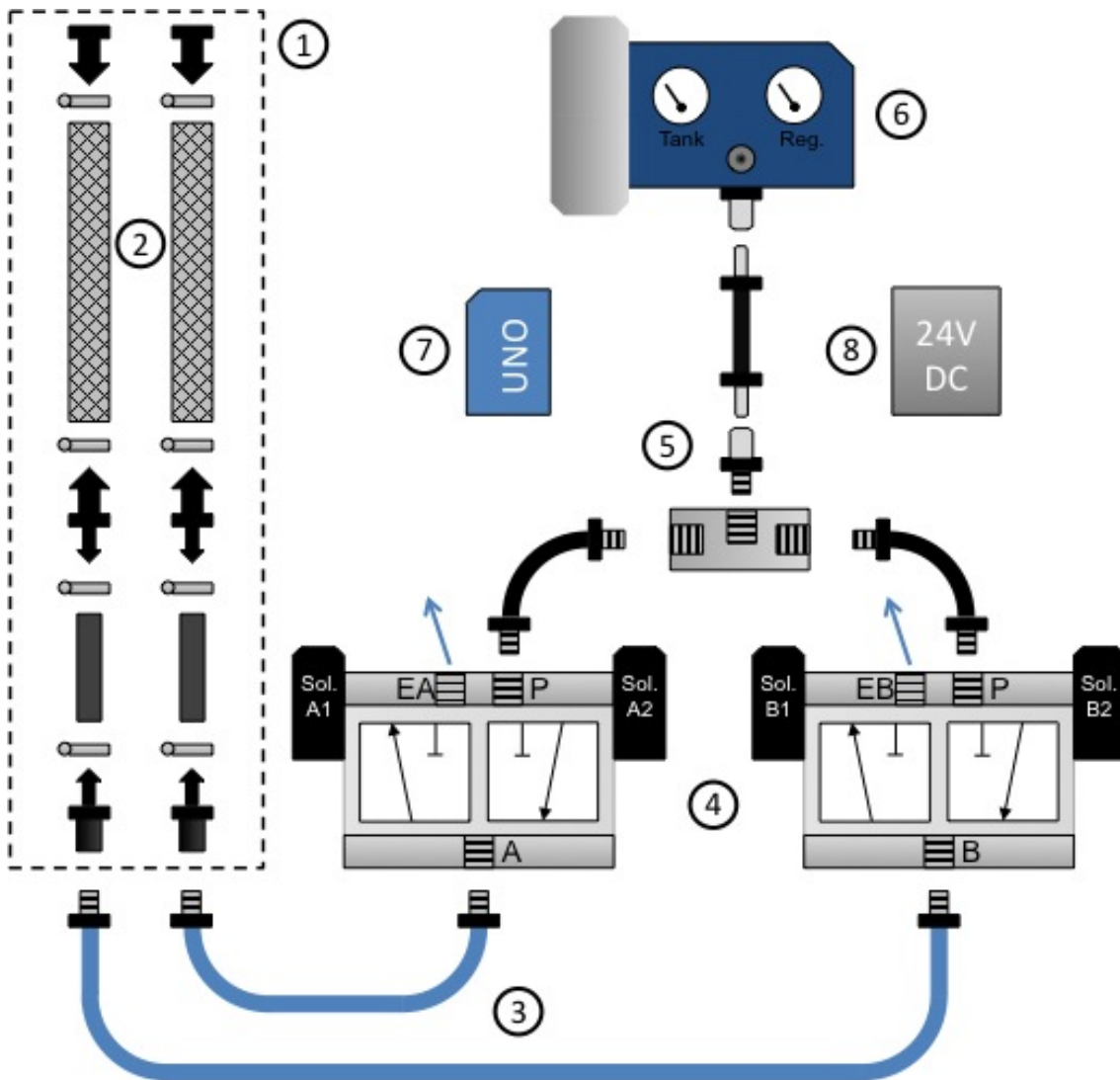


Figure 2.4: Diagram of Final Design Hardware Components.

gait cycle.

3. Lightweight rubber air hoses for transmitting pressurized air from solenoid valves to each of the individual tube actuators on the subject's foot.
4. Three port, two position double-solenoid air control valves for controlling the supply of air pressure to the actuators. The diagrams on each solenoid valve show the two potential positions of the valves.

5. Tee-shaped air hose fitting for supplying both solenoid valves with air pressure from a single air pressure source.
6. Air pressure source for actuating the device, which can be either a pressurized air wall outlet or a portable air compressor depending on the need of the application or scenario.
7. Arduino UNO (or comparable model of Arduino controller) for controlling the actuation of the solenoids in the solenoid valves.
8. DC power supply capable of steady 24V DC supply to solenoids.

The next items to review are those associated to the electrical side of the system. These include the components in Fig. 2.5. The diagram shown in this figure will also serve as a wiring schematic for the fabrication of the control board that interfaces with the Arduino. A description of the main components to the circuit is shown below.

1. TIP122 transistor units with diagrams describing the pin connections with the power supply, Arduino controller, and each individual solenoid.
2. Solenoid valves for each of the four possible valve positions on the two solenoid valve assemblies and diodes placed in parallel to prevent damage from back current.

This concludes the brief review of the various components of the design and their respective roles in operation. A more complete listing of all system components can be found in the system bill of materials (BOM) in Table 2.4. This table also displays the cost of the individual parts that comprise the system in order to get a sense of the required budget. At this point, it is time to start considering the fabrication and assembly of the prototype design.

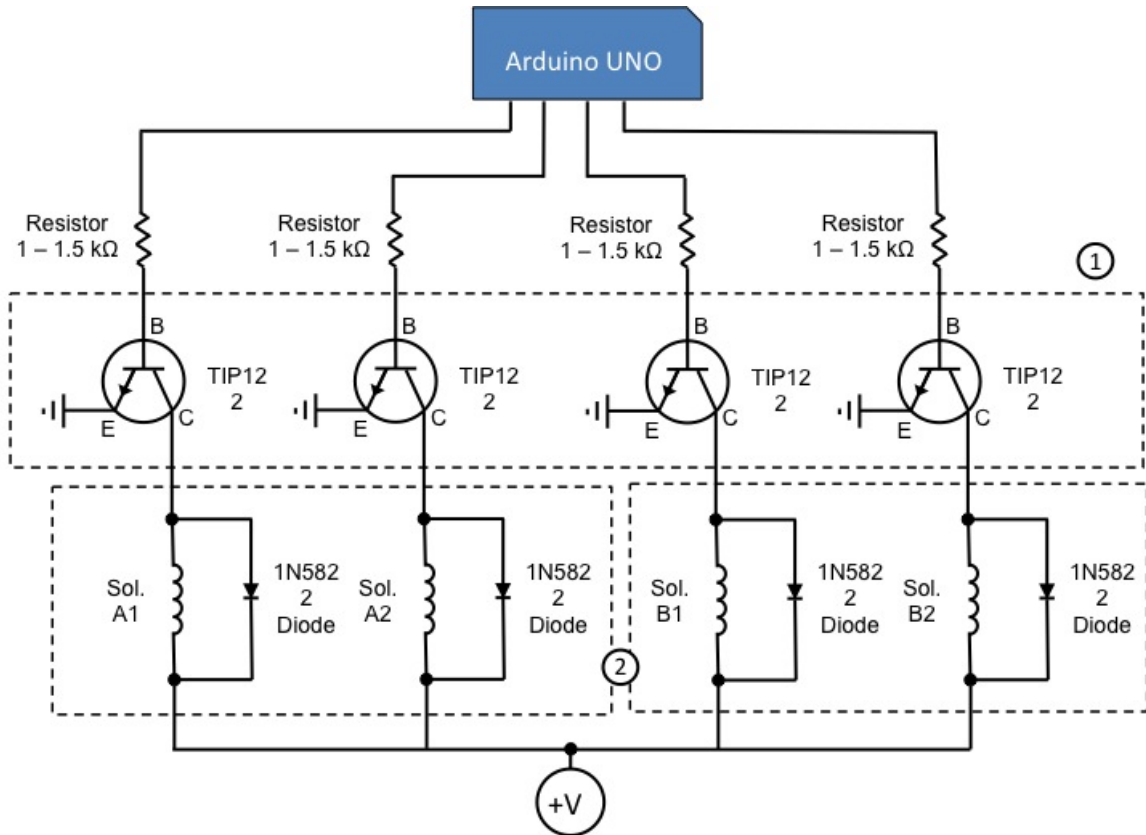


Figure 2.5: Electrical Schematic of Solenoid Control Board.

2.3.2 Fabrication and Assembly

In this section, the components of the design will be fabricated and assembled in order to create a working prototype system. The parts that were discussed previously are ordered from different manufacturing sources and are ready for implementation. However, certain components must be custom fabricated for this application. In particular, the surfaces of the pneumatic device are custom modeled. So far, the material composition of the surfaces has not been specified, but the requirements of the problem will dictate the selection of an appropriate material. Since the system is wearable and must be lightweight, metals and other high density materials are eliminated from the list of possibilities. Another limiting factor is the complex geometry of the design, which prevents many of the more common and conventional machining methods.

Table 2.4: System Bill of Materials.

Part Description	Purpose	Qty.	Cost
Air Directional Control Valve	Controls air flow	2	\$288.98
Tygon PVC Tubing 5/8", 5'	Actuator material	1	\$34.30
Rubber Tubing 3/8", 5'	Connection tubing	1	\$16.50
Straight Barbed Fitting	Tubing transitions	2	\$7.38
Reducing Barbed Fitting(x10)	Tubing transitions	1	\$4.06
Hose Clamps, 1/2"-3/4"(x10)	Seal transitions	1	\$8.41
Hose Clamps, 7/32"-5/8"(x10)	Seal transitions	1	\$5.87
Air Hose, 1/4", 10'	Pressure transmission	2	\$37.28
Air Hose, 1/4", QD, 10'	Pressure transmission	1	\$37.21
Air Hose, 1/4", 1'	Pressure transmission	2	\$23.38
Tee Hose Fitting, 1/4"	Hose transition	1	\$10.71
Ind. Hose Coupling, 1/4"	Source transition	1	\$1.15
TIP122 Transistor(x10)	Solenoid control	1	\$5.36
Diode, 40V, 3A(x10)	Solenoid control	1	\$4.26
TOTAL:	-	-	\$486.00

With all of these factors considered, it would make sense to employ the use of a 3D printer to fabricate the surfaces out of plastic. 3D printing is capable of creating complex geometry with relatively high resolution using lightweight plastics. In addition, the infill can be controlled to adjust the overall rigidity and density of the part being created. Fig. 2.6 shows the models of the front toe and back heel portions of the top surface in the 3D printing software. After some trial prints, the material was chosen to be ABS plastic with a 50% infill based on qualitative assessments of weight

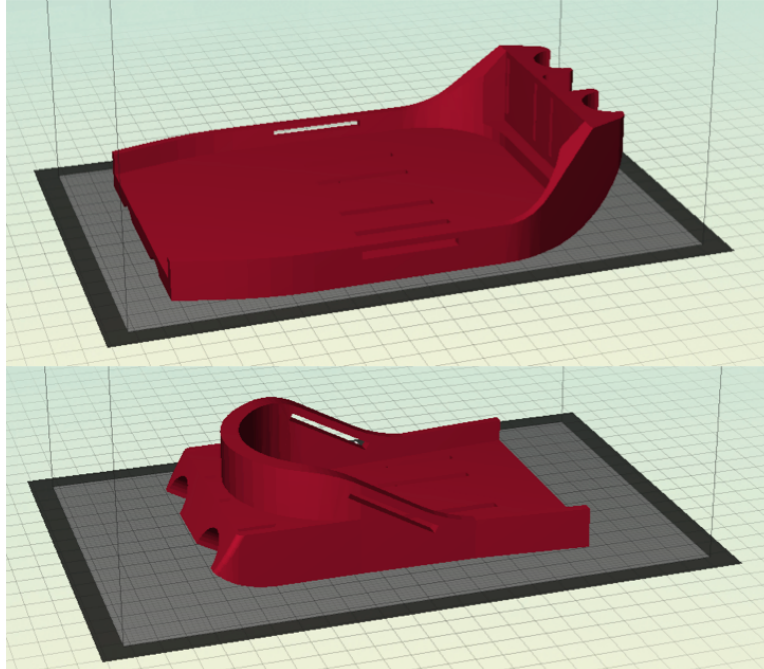


Figure 2.6: Models of Base Components in 3D Printing Software.

and rigidity.

The tube chambers for the actuators are cut to size from the clear tygon tubing material that was purchased. One side of each actuator chamber is sealed with a barbed plug fitting and then secured with an external hose clamp, which is then tightened by hand. The opposite side is transitioned to a smaller diameter rubber tubing section with a reduction barbed fitting and is also secured with an external hose clamp. The next transition is accomplished with threaded 0.25 in barbed fittings to a lightweight rubber air hose, which is then connected to the output of the solenoid valves. All threaded interfaces are assembled with liberal teflon tape to prevent leaks through the seals.

Each actuator tube is secured to the heel and toe surfaces using zip ties. The pressure input side of the actuators is secured at the heel side to reduce the effects of added inertia from the tubes. Relative locations of the surface components on the actuator tubes depend on the individual foot length of the subject. The goal of this

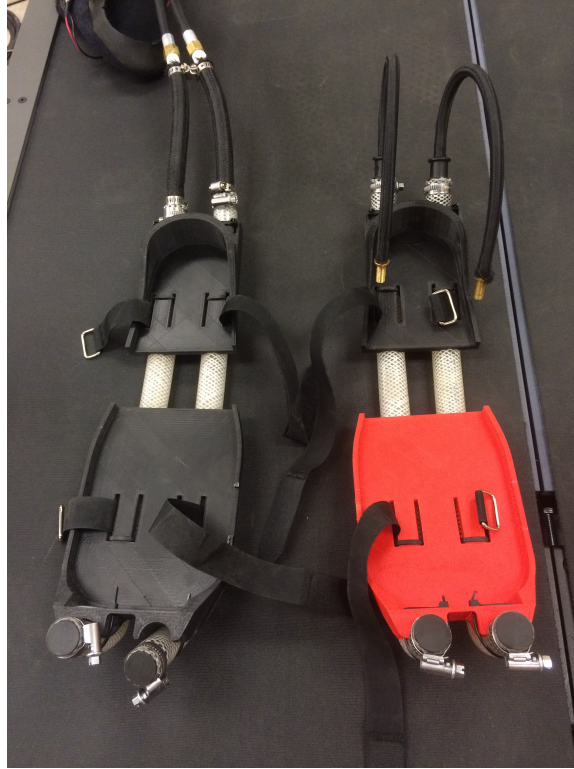


Figure 2.7: Full Assembly with Nonoperational Assembly.

prototype is to use it in inter-leg coordination experiments, so only one fully functional assembly is required to perturb the one side of the body. The opposite side can be a static nonoperational copy of the actuated assembly. While the nonoperational copy of the device has the same surface and actuator tube assemblies, it will not be connected to the solenoid valve pressure source. Instead, it can be pressurized with the bicycle pump using Schrader valves. The two assemblies are shown in Fig. 2.7.

After completing the pneumatic circuit by connecting the other air hose components to the solenoid valves and the pressure source, the pneumatic components are ready for pressurization from the chosen pressure source. The solenoid valve assemblies with associated air hoses can be seen in Fig. 2.8. Before pressurized trials can commence, the solenoids must be wired and tested for proper electrical connections. Each solenoid has a DIN-type connection with three pins. These electrical connec-

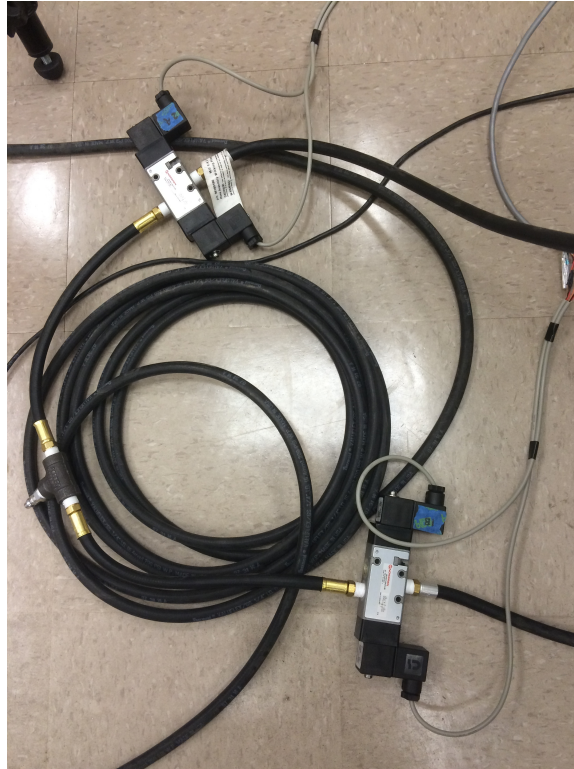


Figure 2.8: Solenoid Assemblies in Pneumatic Circuit.

tions are fed through wires and then consolidated for connection to the custom-made control circuit.

Testing of the solenoids requires the completion of the electrical circuit displayed in the schematic of Fig. 2.5. The construction of this circuit requires great care to ensure that all electrical connections are correct and that no shorts are present. After soldering the electrical components on to the board, an adjustable DC power supply can be connected to test the solenoid actuation. For testing purposes, the Arduino MEGA is connected to the control board, and a simple Arduino code is used to read serial input from a connected computer and send control signals to the transistors. The actuation of the solenoids can be controlled directly from keyboard entries on the connected computer. Upon adding pressure and power to the system, the actuator tubes inflated without leaks, and it was concluded that the pneumatic and electrical

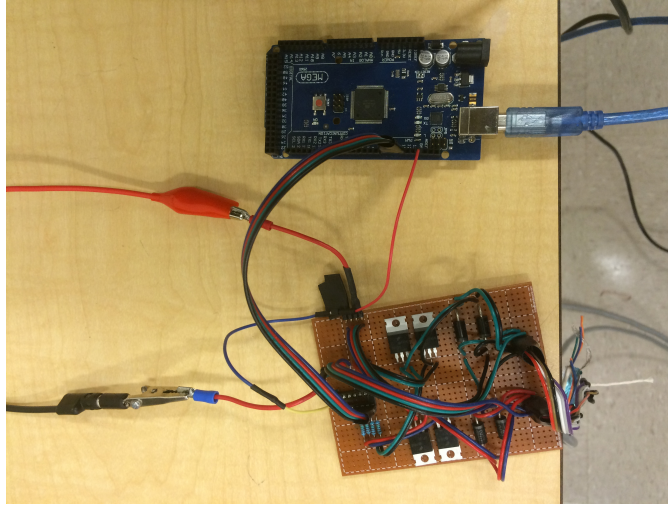


Figure 2.9: Electrical Hardware with Transistors and Arduino MEGA.

circuits were fabricated successfully. Fig. 2.9 displays the completed electrical circuit and an Arduino MEGA.

The fabrication and assembly processes have now led to an operational prototype device capable of controlling ankle inversion and eversion perturbations. Based on preliminary assessments of operation, the system appears to meet all initial design criteria. A more in-depth analysis of its operation is required in order to fully characterize the success of the design. Pending this characterization, progress can begin toward the development of initial experiments with human subjects using this prototype device. Since the designed system is only a prototype effort, the preliminary experiments will be limited in scope. However, it is expected that the results of human trials will give some critical indications about the design's efficiency and the effects of ankle inversion and eversion on human gait. It is hypothesized that changes will be observed in both muscular activation and gait kinematics as a result of these inversion and eversion perturbations.

Chapter 3

EXPERIMENTATION

3.1 Actuation Testing

The prototype wearable pneumatic device is now fully operational after being successfully assembled. Understanding how it operates in regard to angle output and response time is now extremely important. Initially, a theoretical analysis based on projected dimensions resulted in a range of possible inversion and eversion angles. The system is now well defined in terms of dimensions, and further inspection yields an exact expected angular displacement. The angle can be taken between the height of one fully inflated tube and the hypotenuse of the shoe surface in relation to the ground surface. From this information, the projected angle in either inversion or eversion directions of actuation is around 11° . This information can now be confirmed by actuating the device and gathering data on its transient response.

In order to gather accurate angular data from the device over time, a passive infrared tracking system is implemented. Three markers are placed on the surface of the device in an asymmetric layout so that the tracking system can create and attach a local reference frame to the device. One axis of this local reference frame is aligned with the frontal plane in order to directly measure the associated angular displacement. This data is fed from the tracking system to MATLAB where it is recorded and processed. Both inversion and eversion directions of actuation are tested. A representative subject wears the device and stands in a steady position with weight equally distributed across both feet in order to simulate an experimental scenario. The device is initialized by pressurizing both actuators, and then one of the actuators

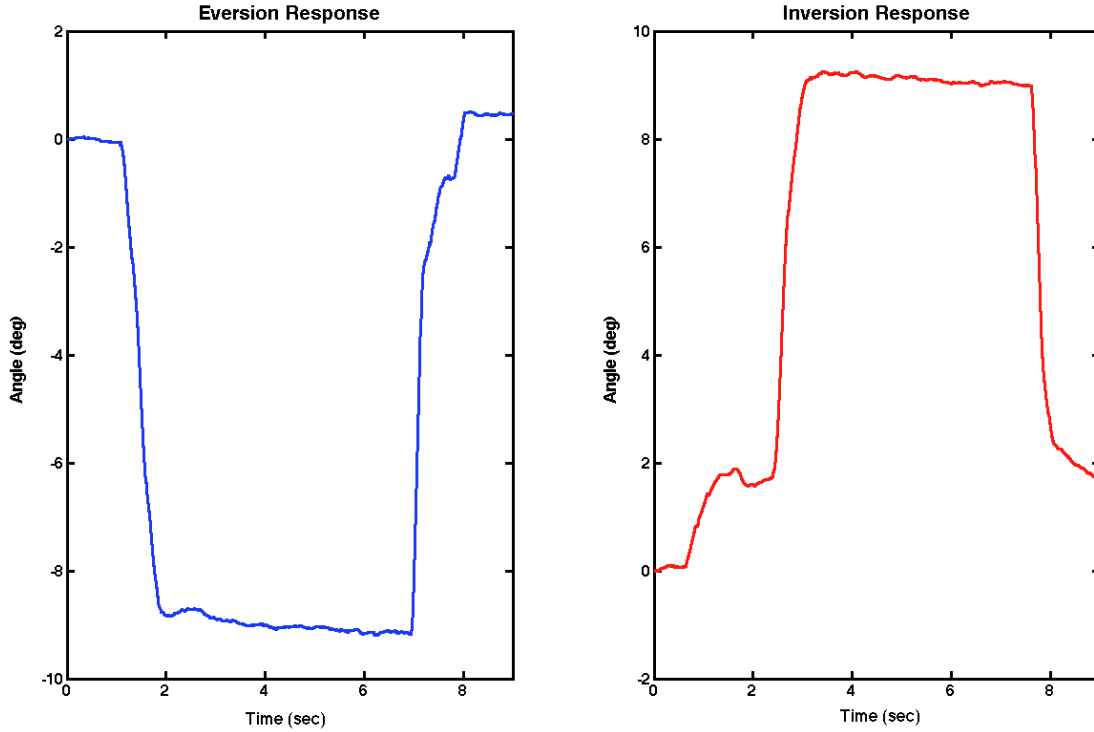


Figure 3.1: Filtered Angle Response Data for Inversion and Eversion

is evacuated to create the actuation in either direction. The results of the experiment are shown in the plots in Fig. 3.1.

This figure shows that the system is indeed successful at creating ankle inversion and eversion. Upon closer examination, it is evident that the magnitude of angular displacement is slightly lower than what was expected. Both inversion and eversion perturbations show angle changes of roughly 9° . The discrepancy between theoretical and experimental values is attributed to any compressibility in the actuators that hasn't been accounted for. The response in Fig. 3.1 also illustrates the amount of time it takes for the system to reach a steady-state angle displacement. For a closer look, the eversion response data was analyzed for rough estimates of settling time and rise time based on an averaged final value. The result is illustrated in Fig. 3.2.

Initial projections indicated that the total time to reach equilibrium pressure would be roughly a tenth of a second, but this analysis neglected the remaining

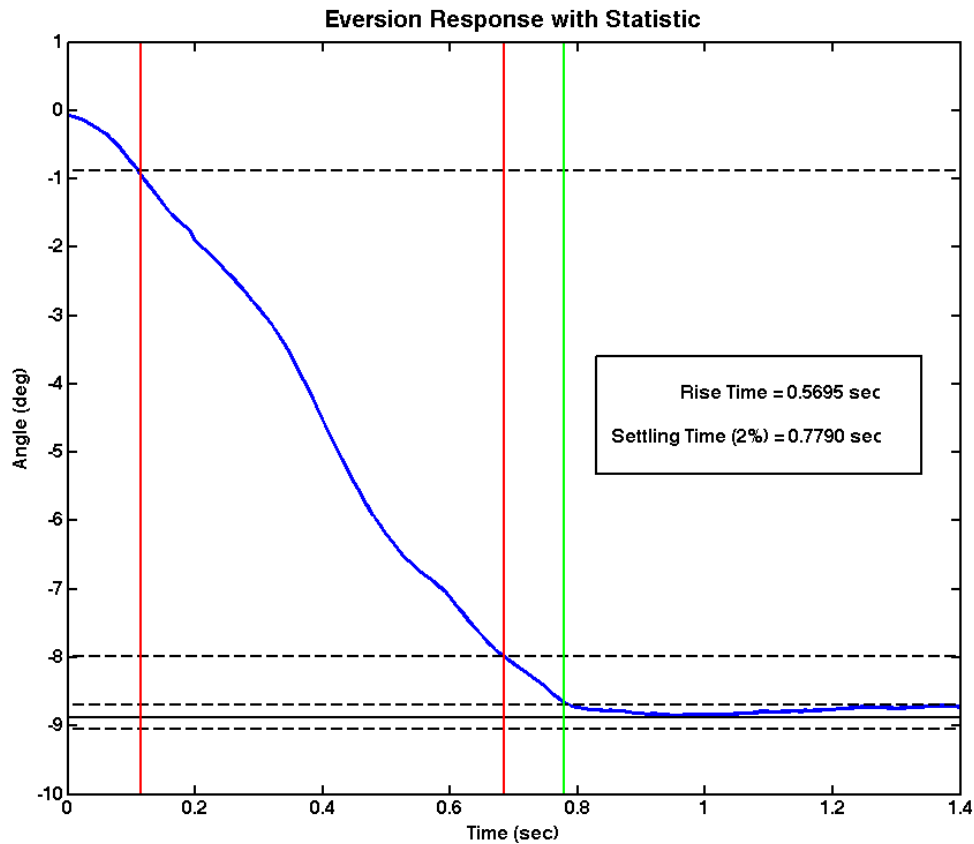


Figure 3.2: Eversion Actuation Response with Statistics.

time that it would take to deflate fully via volume deformation. As these plots demonstrate, this time is not negligible because the total time of response to go from initial pressurized state to final actuated state at 9° is shown to be approximately 0.5 s. While this speed of actuation is reasonable for perturbation experiments, this observation shows that the evacuation time of the actuator tubes should be addressed more carefully in later iterations of the design in order to improve response time.

3.2 Preliminary Experiments

The static actuation test demonstrated that the timely response of the perturbations is adequate, and the overall angular displacement will elicit ankle angle changes

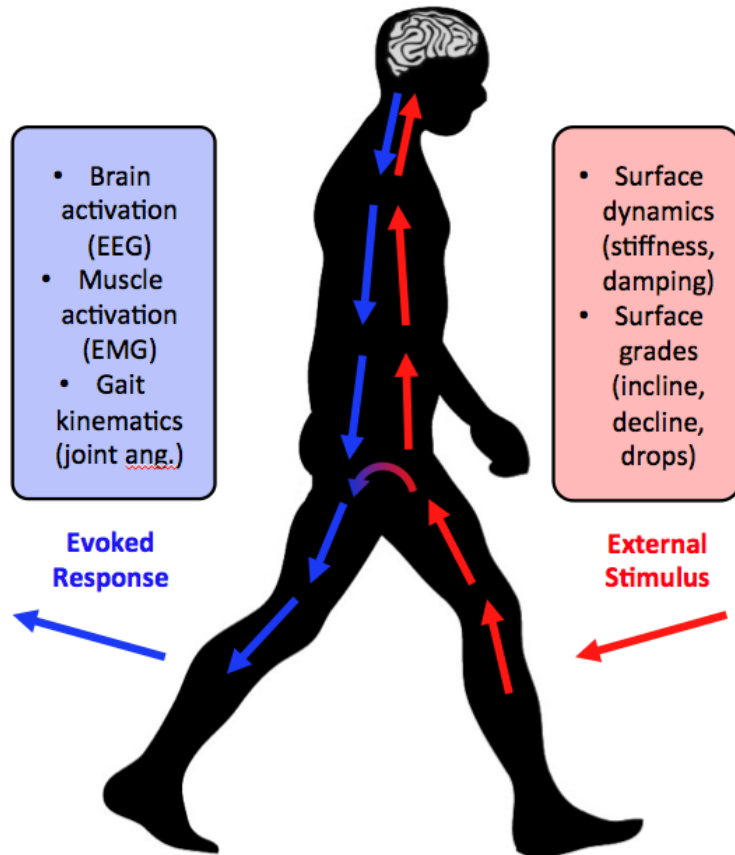


Figure 3.3: Conceptual Illustration of Inter-Leg Coordination.

during the gait cycle. Thus, the prototype system is sufficient for use in experimental scenarios with human subjects. This leads to the necessary development of potential experimental setups. In the discussion of past literature in the introduction of this project, an exciting and novel approach to investigating human gait was presented, which involves the examination of inter-leg coordination mechanisms in relation to surface stiffness changes. This principle of the investigation of inter-leg coordination can be applied using inversion and eversion perturbations as well. The illustration in Fig. 3.3 demonstrates the concept behind the inter-leg coordination investigative approach.

The goal of an inter-leg coordination experiment is to perturb one leg while measuring responses in the contralateral leg. Responses of interest could manifest in gait

kinematics, muscular activation, or brain activation changes. In the context of this investigation, the wearable pneumatic device can be used to create ankle inversion or eversion perturbations during the gait cycle. The measured outcomes will be muscular activation in the form of EMG signals and gait kinematics from the analysis of joint angles. Ankle angle perturbations will be imposed on heel strike of the left leg (or perturbed leg) and will continue through the gait cycle until swing phase of the left leg. Upon entering swing phase, the deflated actuator will be pressurized again in preparation for the next heel strike. The subject's contralateral side will be wearing the nonoperational assembly to ensure gait symmetry. Before the experiment begins, the actuator tubes of this side will be pressurized using a hand pump and will remain at that pressure throughout the experiment.

The subject will be walking on a treadmill with large surface area and handle bars in order to ensure safety. This experiment is covered by the Arizona State University Institutional Review Board (IRB ID#: STUDY00001001). In order to track gait kinematics, pairs of active infrared LED markers are attached to the lower limbs and feet of the subject while being tracked by cameras in the sagittal plane. The relative angles of these pairs of markers can be post-processed to yield joint angles. In cooperation with this system, a set of EMG electrodes are attached to various muscles of interest on the subject's legs. Specifically, this experiment will examine three muscles on each leg including the tibialis anterior (TA), gastrocnemius (GA), and soleus (SOL). A final experiment examined the peroneus longus (PL) muscle as well. These muscles of interest were chosen based on work in previous studies on characterizing ankle responses (Lee *et al.* (2014)).

The timing of perturbations during the gait cycle will remain constant throughout the experiment. However, the type of perturbation—either inversion or eversion—will vary with a total of 25 perturbations of each type. These two different types of

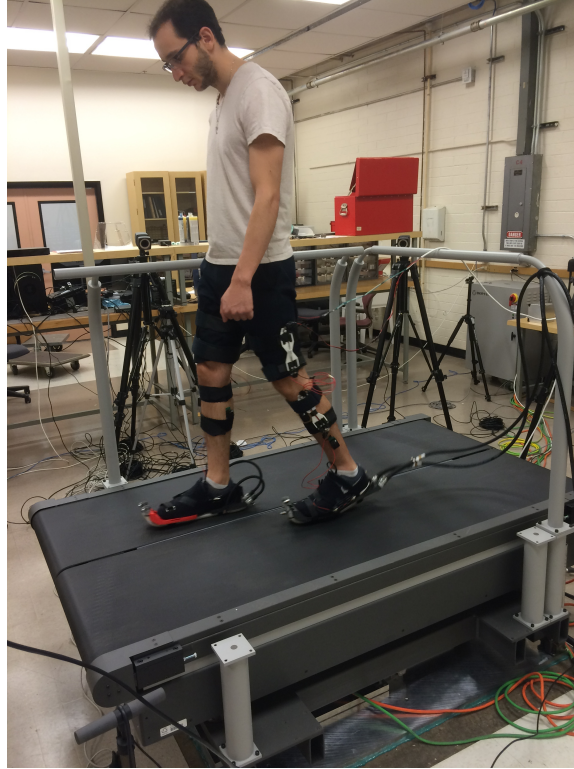


Figure 3.4: Experimental Setup and Subject Wearing Pneumatic Device.

ankle angle perturbations will be distributed randomly throughout the unperturbed cycles of the experiment. To get a baseline of the subject's kinematics and muscular activation without perturbation, there will be an initial phase of approximately 30 unperturbed gait cycles before the perturbations begin. Fig. 3.4 shows the experimental setup that was just discussed.

This experiment was conducted on three different subjects, and the results were processed and analyzed individually. The data on gait kinematics includes joint angles for hip, knee, and ankle in the sagittal plane as a function of gait cycle percentage for the three subjects. Muscular activation data includes EMG signals for TA, GA, and SOL muscles as a function of gait cycle percentage for the three subjects with an additional PL EMG signal data set for the third subject. Both the data on gait kinematics and the data on muscular activation are divided into categories of inversion

perturbations, eversion perturbations, and no perturbations. The figures that follow on the next few pages illustrate data from representative subjects in the study. Fig. 3.5 and Fig. 3.6 show gait kinematics of the second subject for the right and left legs respectively, and Fig. 3.7 and Fig. 3.8 show muscular activation of the third subject for the right and left legs respectively.

The dotted lines shown beneath the plots of muscular activation for the third subject represent statistically significant deviation of perturbed gait cycle data from unperturbed gait cycle data for both inversion and eversion perturbations. Statistical significance was determined based on a two sample t-test. Upon initial observation of these figures, it is apparent that the more interesting results can be found in the muscular activation data while the gait kinematics appear to be unaffected by the perturbations. This conclusion and further discussion of the results from both the response characterization and the preliminary human experiments will be covered in the next sections.

Kinematics: Unperturbed (Right) Leg: Inversion/Eversion Experiment - Subject 2

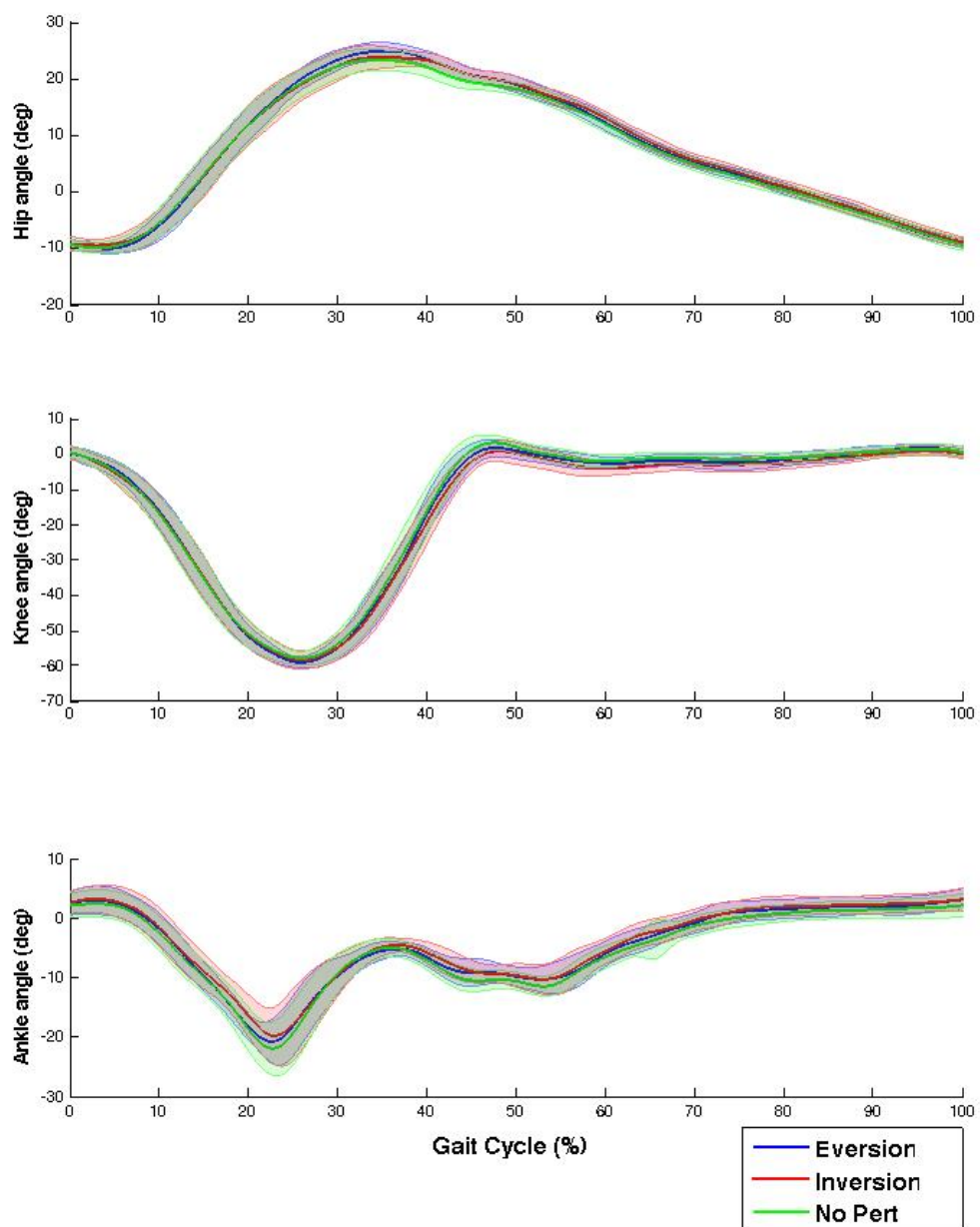


Figure 3.5: Joint Angles of Unperturbed Leg for Representative Subject.

Kinematics: Perturbed (Left) Leg: Inversion/Eversion Experiment - Subject 2

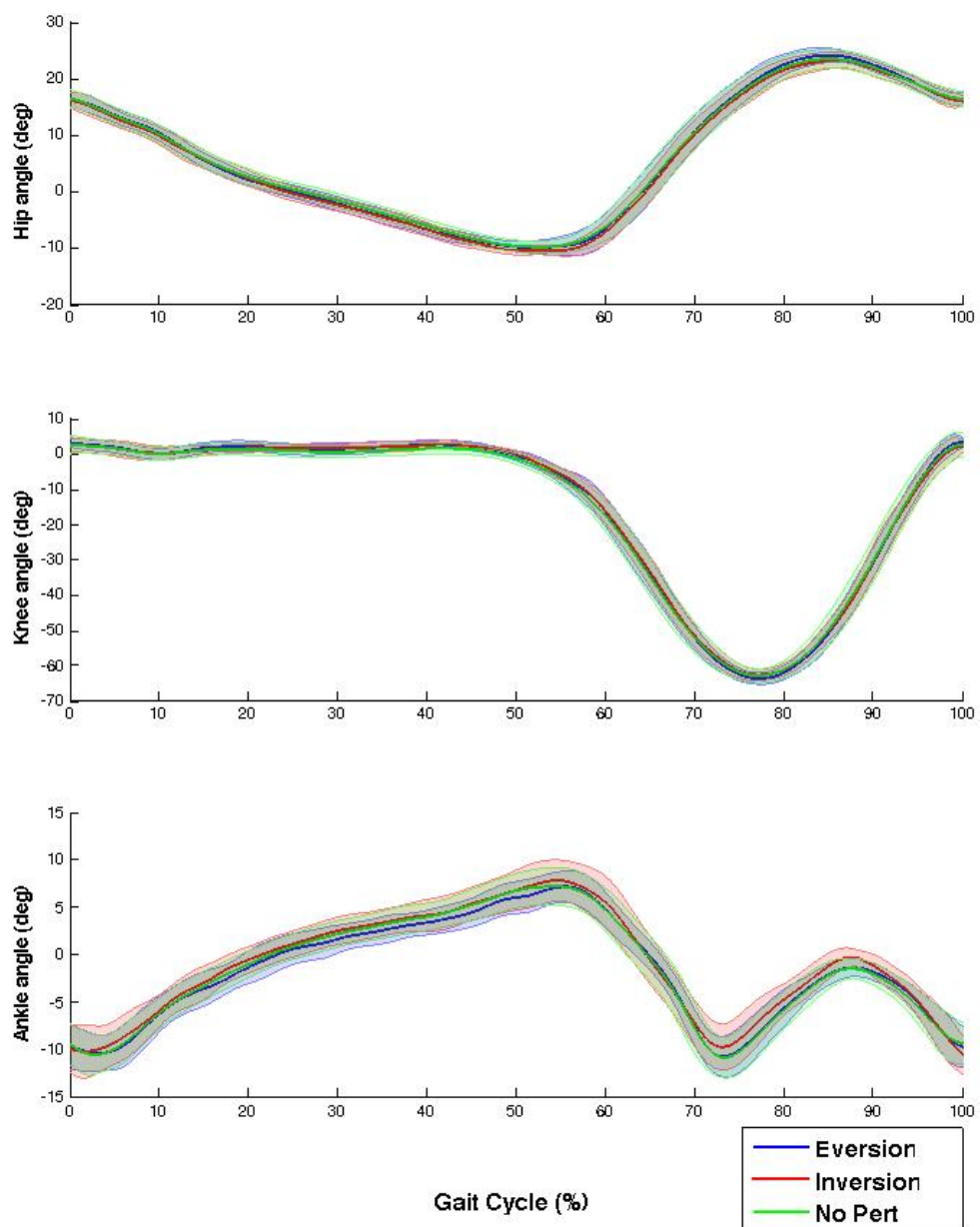


Figure 3.6: Joint Angles of Perturbed Leg for Representative Subject.

Muscles: Unperturbed (Right) Leg: Inversion/Eversion Experiment - Subject 3

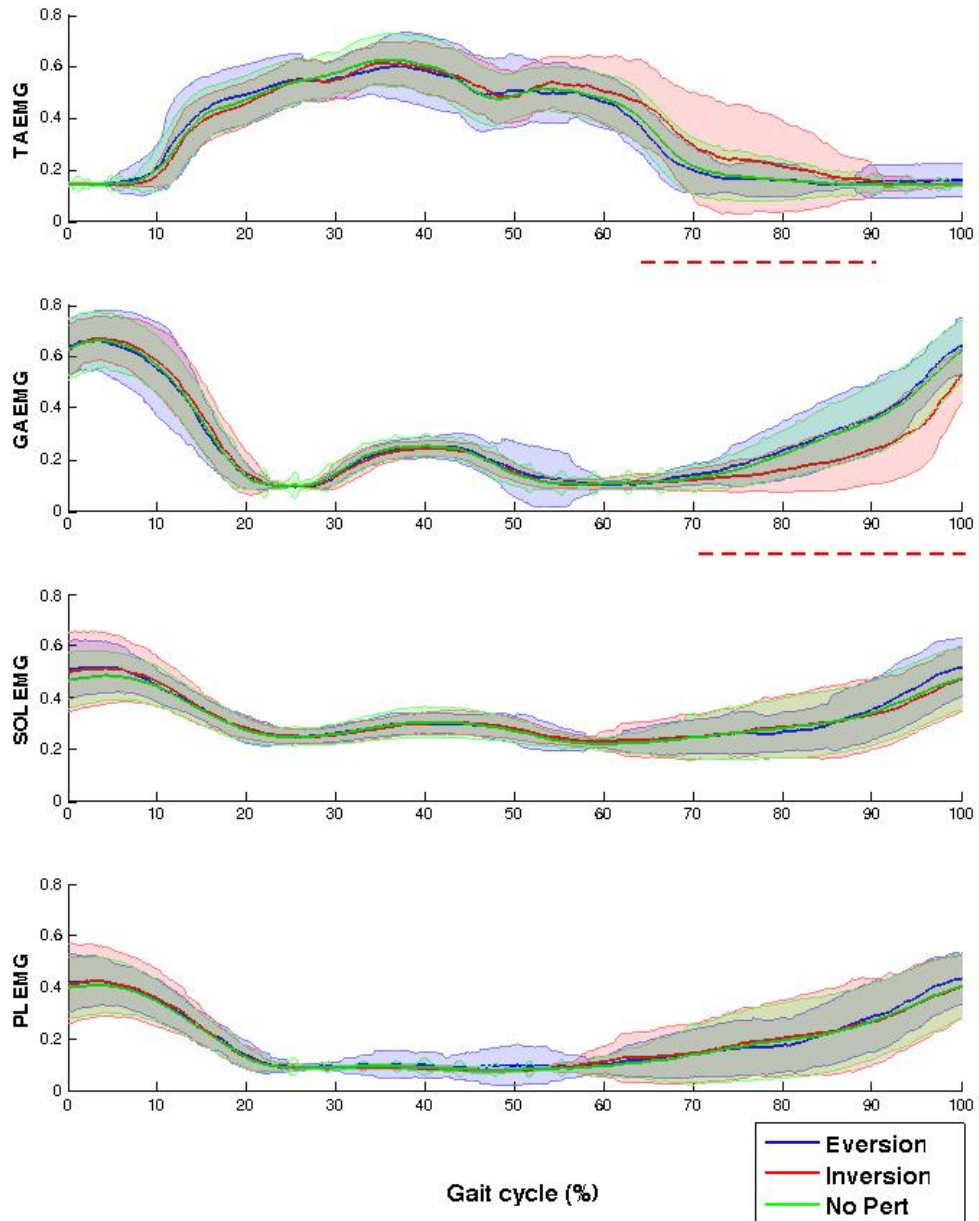


Figure 3.7: Muscular Activation of Unperturbed Leg for Representative Subject.

Muscles: Perturbed (Left) Leg: Inversion/Eversion Experiment - Subject 3

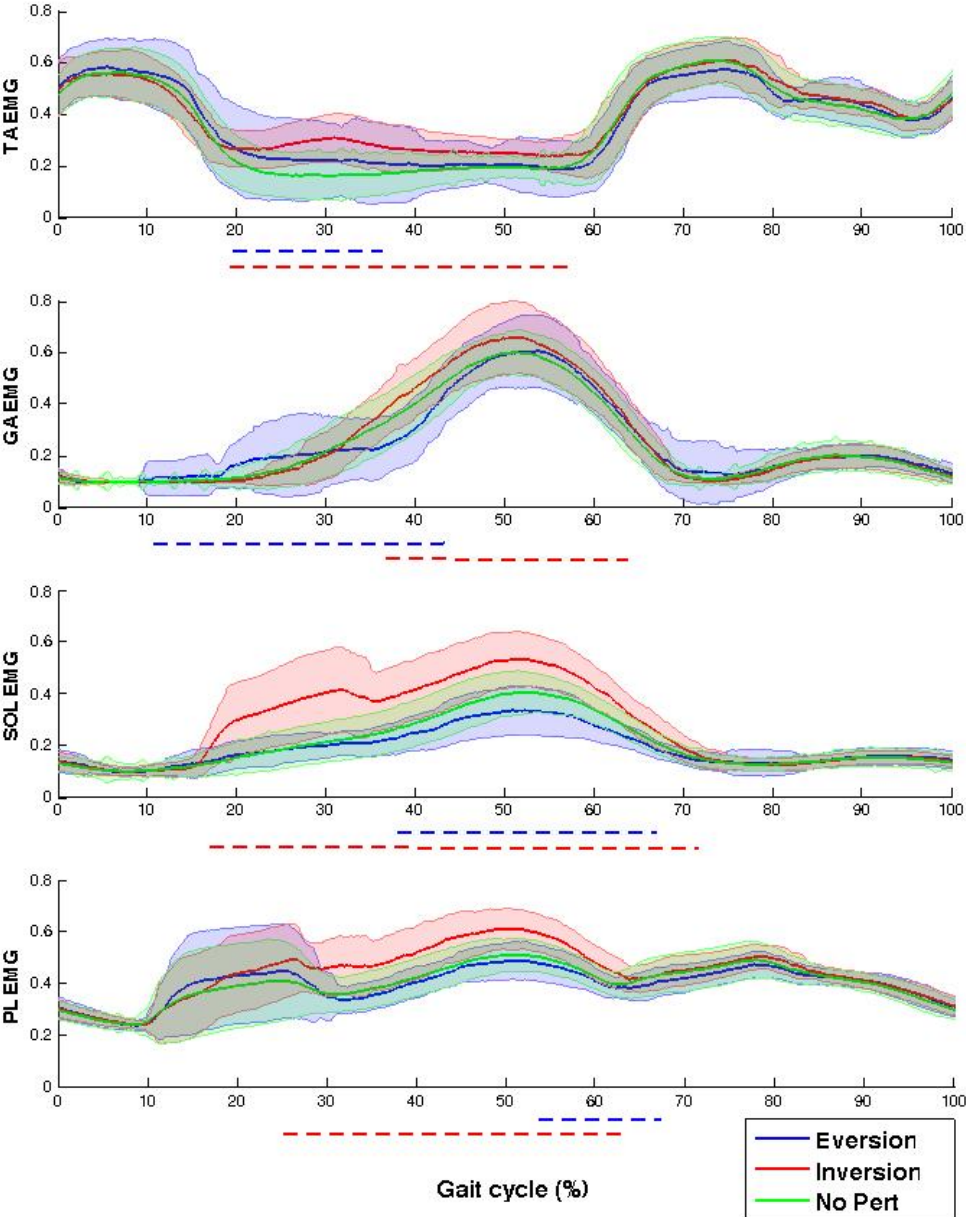


Figure 3.8: Muscular Activation of Perturbed Leg for Representative Subject.

Chapter 4

DISCUSSION

4.1 System Performance

In this section, the performance of the design will be analyzed and discussed in reference to the results of the actuation test and the operation of the device in human trials. The system is designed to be a wearable pneumatic device for investigating ankle inversion and eversion in human gait. In this respect, multiple tests and experiments have confirmed that the prototype design is fully capable of creating consistent inversion and eversion perturbations during the gait cycle. That being said, there are also some aspects of the system's performance that indicate problems in the design of the prototype.

Overall, the system appears to meet all initial design criteria defined in the beginning of the design process—the most important of which being the creation of inversion and eversion ankle angle perturbations. The transient response data for both types of actuation showed inversion and eversion angle changes of around 9° with reasonably quick responses of approximately 0.5 s. The prototype system is extremely lightweight because of its pneumatic mechanism of actuation and low density materials. These aspects in addition to its inherent flexibility make it effective as a wearable device. Furthermore, subjects who were instrumented with the device for preliminary experiments reported that the device did not seem to impede their natural gait motion. Its consistent operation and robust construction ensures safety during experiments as well. The control interface has virtually no processing involved with its operation, and it can be seamlessly interfaced with computer-based data gathering

equipment for easy cooperation with experimental setups. As an added feature, this system can be adjusted to fit a wide range of foot sizes because of its modular design.

Although the tests conducted with this prototype device were largely successful in proving the effectiveness of the design, certain outcomes indicated flaws in the approach that could be addressed in subsequent iterations. While the response time measured in the actuation tests was adequate for preliminary human experiments, the speed of actuation should be increased if the system is to simulate surface angle perturbations as accurately as possible. Even small latencies in the perceived surface angle might result in meaningful differences in human gait responses. Faster response times could be accomplished by increasing the flow rate of the solenoid valves in order to accommodate quicker evacuation. Another potential factor that could influence subject perception of surface angle perturbations is the compliance of the device. The actuator tubes do show minimal displacement especially at heel strike when the impact force of the foot causes the tube to be compressed. Higher operating pressures might yield more rigidity under the load of a human subject.

In general, the system operates as intended, so the design process can be considered a success. Additionally, the possibility of future iterations on the design show promise for improvements in perturbation speed and reductions in unnatural stimulus.

4.2 Preliminary Observations

4.2.1 *Effects on Muscular Activation and Gait Kinematics*

Preliminary experiments with healthy human subjects showed that the prototype system is consistent and effective enough to be employed in experimental applications for the investigation of human gait. The scope of these experiments is limited in size and breadth due to the prototype nature of the design. With that in mind, the gait

kinematics and muscular activation data from these experiments can be analyzed for useful conclusions on characteristic gait responses to inversion and eversion perturbations. This discussion will be referring primarily to the data shown in Fig. 3.5 through Fig. 3.8.

In terms of qualitative notes, there were several important observations made during these preliminary experiments. Across all subjects, the wearable pneumatic device did not appear to have any negative effects on the natural gait motion of the user. Symmetry of gait was a concern in unperturbed gait cycles due to the difference in the operational and nonoperational assemblies on the left and right feet of the subject respectively, but there were no clear signs of asymmetry. Another critical observation was the possible effects of audio cues to the perturbations. Since the prototype system's exhaust makes noise, subjects may have received warning of an imminent perturbation on the upcoming heel strike. While the direction of perturbation was still unknown, the subjects may have prepared for the heel strike in some manner that could have affected the data.

The first topic in the discussion of the resultant data is the observed effects on gait kinematics. Upon examination of the data shown in Fig. 3.5 and Fig. 3.6, there does not seem to be any obvious change in joint angles across either type of perturbation for both the unperturbed and perturbed legs. The trend in these results is common across all three subjects in the experiment. This leads to the conclusion that gait kinematics in relation to inter-leg coordination mechanisms are not significantly influenced by inversion and eversion surface angle perturbations. After evaluating this conclusion further, these results make sense due to the fact that the joint angle outcomes being measured are all in the sagittal plane of the subject's body. The perturbations created from the prototype device cause angle changes in the frontal plane. Therefore, more conclusive evidence of kinematic changes from

inversion and eversion ankle angle perturbations might be found in frontal plane motion as a function of balance coordination mechanisms.

This leads to the discussion of the results in changes of muscular activation. As illustrated by the statistical significance indicators below each plot in Fig. 3.7 and Fig. 3.8, there is certainly some quantifiable effect in muscular activation from the imposed perturbations. This effect seems to be more associated with the perturbed leg rather than the unperturbed leg, which is contrary to what was hypothesized for this inter-leg coordination experiment. The data from subject three shows the greatest effects, but this particular phenomenon of muscular activation changes in the perturbed leg appears in subjects one and two as well. When examining the EMG signal discrepancies more closely, it can be observed that the changes in activation coincide at the instant following the heel strike perturbation as the perturbed leg follows through with mid stance phase of the gait cycle. In particular, activations from the inversion perturbations are pronounced, and these effects seem to propagate across all of the muscles. The most significant change is shown in the activation of the SOL muscle of the perturbed leg during inversion perturbations. Inversion perturbations cause the foot to turn in, which might have the effect of extending the soleus muscle. One might conclude that this stimulus causes the body's gait mechanisms to resist this motion by increasing soleus activation. This logic can also be extended to the increased activation seen in the peroneus longus muscle, which also acts to evert the ankle.

On the contralateral side of the body, the effects are not nearly as strong. One interesting aspect to note is the increased activity of the TA muscle in the unperturbed leg upon the unperturbed leg's heel strike after a perturbation. This effect seems to show that there is an expectation of the body to encounter an off-angle surface. Hence, the TA muscle will increase activation in order to lift the toe and prepare

for an uneven impact. Besides this observation, the data suggests that surface angle perturbations in the frontal plane do not correlate with any significant responses in the contralateral leg as a function of inter-leg coordination mechanisms.

Generally speaking, these conclusions must be validated further with more experiments and scrutinization, but the fact that inversion and eversion perturbations have an observable effect on muscular activation is encouraging for future applications of this technology. As such, the prototype device demonstrates merit for continued investigation of gait mechanisms in relation to surface angle changes and the characteristic responses of the human body during gait.

4.2.2 *Comparison of Inversion and Eversion*

To further this discussion of observed muscular activation changes, it might also be useful to examine the differences in results between inversion and eversion perturbations in order to compare and contrast their effects. It was concluded previously that the increased activation of the SOL and PL muscles of the perturbed leg during inversion perturbations might be indicative of preventative measures by gait mechanisms to oppose the motion caused by these perturbations. It might also be possible to apply this conclusion to the opposite case for eversion. The muscular activation of the GA muscle of the perturbed leg exhibits the same type of increase upon heel strike when the everted surface angle is encountered, but the GA muscle being measured is on the inside of the leg and acts to invert the ankle. At this point, a clearer picture is being developed of the responses to these types of perturbation. Essentially, the muscles that actuate the ankle in the frontal plane act to invert or evert the ankle in order to stabilize the foot in the opposite direction of the perturbation.

Taking this comparison even further, the data in Fig. 3.7 and Fig. 3.8 shows that certain areas actually indicate decreased activation of muscles that aren't opposing

the ankle angle changes. This effect can be observed in the lowered activation of the SOL during eversion perturbations in the perturbed leg. Since the ankle motion is shortening the SOL muscle in the process of the eversion perturbation, the body does not need to activate it as much for stabilization purposes.

To contrast the two types of perturbations, it does seem as though the surface angle perturbations that cause inversion have a much more noticeable effect on muscular activation. It is hypothesized that this trend might indicate more inherent instability caused by the inversion of ankles, which corresponds to a heightened effort by the body to counteract the perturbation. While in the case of eversion, the body is more conditioned to the disturbance, and stability is more easily maintained.

Chapter 5

CONCLUSION

To summarize, the goal of this project was to design, fabricate, test, and implement a novel device for investigating ankle inversion and eversion in human gait. The various stages of the design process yielded a prototype wearable pneumatic device that met all of the necessary design requirements in addition to having the added feature of acting passively on the body. In testing and characterization, this device performed adequately and showed reasonable consistency with expected measures of operation, which were based on theoretical analysis. The actuation test showed a response time of approximately 0.5s and an angular displacement of 9° for both inversion and eversion actuation types.

After the system testing phase, the prototype was implemented in an experiment investigating the effects of inversion and eversion ankle angle perturbations on inter-leg coordination mechanisms in healthy human subjects. The outcomes of this experiment demonstrated that gait kinematics were largely unaffected by the surface angle perturbations created by the prototype device. On the other hand, data from muscular activation of the perturbed leg showed varying levels of statistically significant changes in TA, GA, SOL, and PL EMG signals. Early speculations on the trends of this data suggest that there are active gait mechanisms that work to oppose the motions caused by surface angle perturbations in order to promote mid stance stability in the perturbed leg. Contrary to expectations, the contralateral leg did not demonstrate changes in muscle activation that were significantly different from the unperturbed cases, so it was determined that inter-leg coordination mechanisms were not triggered by the surface angle perturbations.

In conclusion, the successful design and implementation of this wearable pneumatic device has resulted in some interesting findings related to the effects of ankle inversion and eversion on human gait. These results, especially in relation to the limited scope of the experiments conducted in this study, are encouraging for the potential application of this prototype device in future investigative ventures. After further design iterations, the device could be an extremely useful tool for characterizing human gait responses to ankle inversion and eversion.

REFERENCES

- Andersen, J. B. and T. Sinkjaer, “An actuator system for investigating electrophysiological and biomechanical features around the human ankle joint during gait”, *IEEE Transactions on Rehabilitation Robotics* **3**, 4, 299 – 306 (1995).
- Begeman, P., P. Balakrishnan, R. Levine and A. King, “Dynamic human ankle response to inversion and eversion”, *SAE Technical Paper* (1993).
- Farris, D. J. and G. S. Sawicki, “The mechanics and energetics of human walking and running: a joint level perspective”, *Journal of the Royal Society Interface* (2011).
- Hornby, T. G., D. Cambell, J. H. Kahn, T. Demott, J. L. Moore and H. R. Roth, “Enhanced gait-related improvements after therapist-versus robotic-assisted locomotor training in subjects with chronic stroke”, *Stroke* **39**, 1, 1786 – 1792 (2008).
- Lee, H., H. I. Krebs and N. Hogan, “Multivariable dynamic ankle mechanical impedance with relaxed muscles”, *IEEE Transactions on Neural Systems and Rehabilitation Engineering* **22**, 6, 1104 – 1114 (2014).
- Nakazawa, K., N. Kawashima, M. Akai and H. Yano, “On the reflex coactivation of ankle flexor and extensor muscles induced by a sudden drop of support surface during walking in humans”, *Journal of Applied Physiology* **6**, 2, 604 – 611 (2003).
- Nardone, A., T. Corra and M. Schieppati, “Different activations of the soleus and gastrocnemii muscles in response to various types of stance perturbation in man”, *Experimental Brain Research* **80**, 2, 323 – 332 (1990).
- Prentice, S. D., E. N. Hasler, J. J. Groves and J. S. Frank, “Locomotor adaptations for changes in the slope of the walking surface”, *Gait & Posture* **20**, 3, 255 – 265 (2004).
- Roy, A., H. I. Krebs, D. J. Williams, C. T. Bever, L. W. Forrester, R. M. Macko and N. Hogan, “Robot-aided neurorehabilitation a novel robot for ankle rehabilitation”, *IEEE Transactions on Robotics* **25**, 3, 569 – 582 (2009).
- Skidmore, J., A. Barkan and P. Artemiadis, “Variable stiffness treadmill (vst): System development, characterization and preliminary experiments”, *IEEE Transactions on Mechatronics* **20**, 4, 1717 – 1724 (2014).